Mechanoreciprocity requires interactions between TRPV4 channels, the Rho pathway and actin cytoskeleton

Monika Lakk,[1] David Križaj[1-3]

From the [1]Departments of Ophthalmology & Visual Sciences; [2]Bioengineering; [3]Neurobiology & Anatomy, University of Utah, Salt Lake City, UT

Corresponding authors: Monika Lakk or David Krizaj, 65 N Mario Capecchi Drive, Bldg. 523, Room S4140 JMEC, Salt Lake City, UT 84132. Email: mlakk@gamma.ttk.pte.hu; david.krizaj@hsc.utah.edu

Running title: Mechanoreciprocity in trabecular meshwork cells

Keywords: Trabecular meshwork, glaucoma, TRPV4, calcium, integrin, focal adhesion, actin, paxillin, zyxin, cyclic stretch, mechanoreciprocity, glaucoma

ABSTRACT

Intraocular pressure (IOP) is dynamically regulated by the trabecular meshwork (TM), a mechanosensitive tissue that protects the eye from injury through dynamic regulation of aqueous humor outflow from the anterior chamber of the eye. IOP-dependent increases in TM stiffness and contractility drive open angle glaucoma but the mechanotransduction mechanisms that regulate these processes remain poorly understood. We used fluorescence imaging and biochemical analyses to investigate cytoskeletal and focal adhesion remodeling in human TM cells stimulated with cyclic strain. The cells showed enhanced F-actin polymerization, increased number and size of focal adhesions, and activation of the Rho-associated protein kinase (ROCK). Stretch-induced activation of the small GTPase RhoA, and tyrosine phosphorylations of focal adhesion proteins paxillin, focal adhesion kinase (FAK), vinculin and zyxin were time-dependently inhibited by HC-067047, an antagonist of transient receptor potential vanilloid 4 (TRPV4) channels, and the ROCK inhibitor Y-27632. TRPV4 and ROCK activation were required for zyxin translocation and increase in the number/size of focal adhesions in stretched cells. Y-27632 blocked actin polymerization without affecting calcium influx induced by membrane stretch and the TRPV4 agonist GSK1016790A. These results reveal that mechanical tuning of TM cells requires parallel activation of TRPV4, integrins and ROCK, with chronic stress leading to sustained remodeling of the cytoskeleton and focal complexes.

Introduction

The ability of eukaryotic cells to change their cytoskeleton in response to the mechanical environment is critical for a wide range of biological and pathological processes (1, 2). In general, application of tensional forces across the lipid bilayer of nonexcitable cells triggers calcium influx via stretch-activated channels (SACs), with Ca^{2+} signaling mediating activation of myosin light chain kinases (MLCKs), inactivation of MLC phosphatases (MLCPs), disinhibition of caldesmon-dependent myosin ATPases and Rho (Ras homology) GTPases, and activity of nonmuscle myosins (3-5). Calcium-mediated phosphorylation of MLC drives formation of contractile actomyosin units and stress fibers, which exert force on integrins, their cytoskeletal anchoring proteins and modulate downstream pathways such as Rho GTPase-dependent modulation of Rho-associated kinase (ROCK) and LIM kinases (6). SACs, the cytoskeleton and contractility shape the structural and functional plasticity of cells exposed to mechanical stress through focal adhesions (FAs), macromolecular assemblies organized around integrin core that bidirectionally transmit tensile forces between the extracellular matrix (ECM) and the cytoskeleton (6-8). Exertion of mechanical forces across FAs increases the accessibility of the cytosolic integrin tail to actin-binding proteins and induces tyrosine phosphorylations of key FA proteins such paxillin, focal adhesion kinases (FAKs) and vinculin (7, 9, 10) to augment the cells' resistance to mechanical stress ('mechanoreciprocity'). Ridley and Hall (1992) showed that active RhoA induces formation of stress fibers and FAs but whether and how SACs interact with the Rho pathway and FAs in the presence of forces is not known.

The biomechanical milieu in the vertebrate eye is dominated by intraocular pressure (IOP), which maintains its shape, regulates development of ocular tissues and modulates cellular signaling. IOP is dynamically controlled by the trabecular meshwork (TM), a layered tissue composed of contractile smooth muscle (SM)-like cells populating ECM beams that are anchored to the endothelial cells lining the canal of Schlemm. Mechanical stretch evokes TM contractions (11), thereby increasing the tissue resistance to aqueous humor drainage to elevate IOP (12, 13). At the cellular level, TM cells compensate

for pressure-evoked strains with remodeling of cytoskeletal and ECM pathways that inhibit their ability to drain aqueous humor (14). This process becomes dysfunctional in hypertensive glaucoma, as TM cells lose the capacity for homeostatic regulation and adopt the myofibroblast phenotype characterized by increased actin polymerization, α–smooth muscle actin (αSMA) expression, deposition of ECM, and transforming growth factor β (TGFβ) release (14-17). Overall, continued exposure to mechanical stress makes the TM stiffer and more contractile, thereby maintaining IOP in a vicious circle that may result in optic neuropathy (18-20). The remodeling process and IOP elevations in humans and animals with open angle glaucoma can be countered with actin depolymerizers and ROCK inhibitors, which function as IOP-lowering neuroprotective agents in human and animal glaucoma (21, 22). It is therefore of central importance to delineate the molecular mechanisms that drive mechanically induced, Rho-dependent upregulation of TM actin polymerization and contractility.

Here, we tested the hypothesis that force-induced remodeling requires collaboration between transient receptor potential vanilloid isoform 4 (TRPV4), a calcium-permeable polymodal SAC that mediates the responses to strain, swelling, pressure and polyunsaturated fatty acids in TM cells (23-25), and Rho signaling, the actin cytoskeleton and FA pathways. TRPV4 is prominently expressed in mouse and human TM membrane and primary cilia (23, 26) and is often targeted to actin-enriched regions and areas of high strain such as FAs (27-30). In smooth muscle, mesenchymal, and endothelial tissues exposed to mechanical stress and/or TGFβ, TRPV4 promotes myofibroblast transdifferentiation that bears resemblance to TM remodeling in glaucoma (31-34) whereas TRPV4 inhibitors protect against fibrosis (33, 34) and lower IOP in a mouse model of glaucoma (23). We found that physiological strain stimuli promote actin polymerization, phosphorylation and/or translocation of key FA-anchoring proteins through a process that requires coordinated activation TRPV4-mediated Ca^{2+} entry and Rho signaling. These findings thus establish a novel molecular framework that accounts for increased TM stiffness in glaucoma (18), and the efficacy of ROCK/TRPV4 antagonists as IOP-lowering agents in glaucomatous eyes (22, 23).

Materials and Methods

Cell culture. Human trabecular meshwork (hTM cells), isolated from the juxtacanalicular and corneoscleral regions of the human eye (ScienCell Research Laboratories) were cultured in Trabecular Meshwork Cell Medium (ScienCell Research Laboratories) supplemented with 2% fetal bovine serum (FBS), 100 units/ml penicillin, 100 μg/ml streptomycin, at 37 ^{o}C and pH 7.4. In accordance with consensus characterization recommendations (23, 104, 24), the phenotype was periodically validated by profiling for markers *MYOC, TIMP3, AQP1, MGP, ACTA2* (α-smooth muscle actin, αSMA) (Supplementary Figure 6) . The morphology, TRPV4 activation and stretch-induced phosphorylation of FAK and zyxin in hTM cells were virtually indistinguishable from cells dissected from nonglaucomatous donor eyes (56 year old, male and 62 year old, female) (23, 24, 104; Supplementary Figure 7). Human tissues were used in concordance with the tenets of the WMA Declaration of Helsinki and the Department of Health and Human Services Belmont Report. Preliminary accounts of this work were published in abstract form (126, 129).

Reagents. The TRPV4 agonist GSK1016790A (GSK101) and antagonist HC-067047 (HC-06) were purchased from Sigma. GSK101 (1 mM), Y-27632 (20 mM) and HC-06 (20 mM) DMSO stocks were diluted in extracellular saline, with the final drug concentrations not exceeding 0.1%. The ROCK1/2 inhibitor *Trans*-4-[(1*R*)-1-Aminoethyl]-*N*-4-pyridinylcyclohexanecarboxamide dihydrochloride (Y-27632) was obtained from Cayman Chemical and the calcium indicator Fura-2 AM from Life Technologies. Salts were purchased from Sigma or VWR.

Reverse Transcription and Polymerase Chain Reaction (PCR). Total RNA was isolated using Arcturus PicoPure RNA Isolation Kit according to the manufacturer instructions (Applied Biosystems). One microgram of total RNA was used for reverse transcription. First-strand cDNA synthesis and PCR amplification of cDNA were performed using qScript^{TM} XLT cDNA Supermix (Quanta Biosciences). The

RT-PCR products were run on 2% agarose gels and visualized by ethidium bromide staining, along with 100-bp DNA ladder (Thermo Scientific).

Quantitative Real-Time Polymerase Chain Reaction (Q-RT-PCR). SYBRGreen based real-time PCR was performed using Apex qPCR GREEN Master Mix (Genesee Scientific). The experiments were performed as triplicates of at least three independent experiments and are expressed as a ~fold change compared to the control. The C_T method ($\Delta\Delta C_T$) was used to measure relative gene expression where the ~fold enrichment was calculated as: $2^{-[\Delta CT\ (sample)\ -\ \Delta CT\ (calibrator)]}$ after normalization. GAPDH and β-tubulin were utilized as endogenous controls to normalize the fluorescence. The primer sequences are listed in Table 1.

Western Blots. Cells were lysed on ice using a radioimmunoprecipitation assay (RIPA) lysis buffer system (Santa Cruz Biotechnology) containing PMSF, sodium-orthovanadate and protease inhibitor cocktail (Santa Cruz Biotechnology) to avoid degrading processes. An equal amount of protein (20-25 μg) was loaded in 10 or 12 % SDS-polyacrylamide gels. Samples were transferred to polyvinylidene difluoride (PVDF) membranes for 1h at 300 mA. The non-specific binding sites were blocked with 5% non-fat milk and 1% bovine serum albumin (BSA) and incubated overnight at 4 ºC with primary antibodies. Primary antibodies and their specifications are listed in Table 2. The binding of the primary antibodies was quantitated with anti-mouse (1:2000, Life Technologies) or anti-rabbit (1:3000, Cell Signaling) horse-radish peroxidase (HRP)-conjugated secondary antibodies. HRP conjugated anti-rabbit-GAPDH (1:10.000, Abcam) antibody was used as loading control. The blotted proteins were developed using an enhanced chemiluminescence kit (Thermo Scientific).

Rho Activity Assay. GTPase activity was assessed with the Active Rho Detection Kit (Cell Signaling) according to the manufacturer's instructions. Briefly, the assay takes advantage of GTP-bound Rho (active form) binding to the Rhotekin-RBD fusion protein, expressed as a GST-fusion protein in *E. coli*. The protein shows selectivity for GTP-bound as opposed to “inactive” GDP-bound RhoA, RhoB and RhoC isoforms and precipitates active Rho proteins on glutathione resin. The level of activation was quantified with Western blots (the Rho antibody obtained from Cell Signaling was used at 1:500).

Confocal microscopy. Apoptosis assay: cells were pre-incubated with SRB-VAD-FMK, a cell permeable fluorogenic caspase probe (1:250, AAT Bioquest) at 37 °C, 5% CO_2 for 1 hour before fixation. Immunofluorescence: Cells were fixed with 4% paraformaldehyde for 10 minutes and blocked in PBS (5% FBS and 0.3% Triton X-100) for 20 min (124, 127). Alexa Fluor 488 phalloidin (Life Technologies) was utilized for F-actin staining (1:1000 for 1 hr). Primary antibodies (Table 2) were diluted in PBS (2% BSA and 0.2% Triton X-100) and incubated overnight at 4°C. After rinsing, the cells were incubated for 1 hour at RT with goat anti-mouse and goat anti-rabbit IgG (H + L) secondary antibodies were conjugated to fluorophores (Alexa Fluor 488 nm, 568 nm and/or 594 nm; Life Technologies; 1:500). Unbound antibodies were rinsed away and conjugated fluorophores were protected with Fluoromount-G (Southern Biotech) prior to mounting coverslips. The slides were viewed on a confocal microscope (Olympus FX1200) at 1024 x 1024 pixels using a 20X water superobjective (1.00 N.A.; field size: 158.565 x 158.565 µm; 0.155 µm/pixel; sampling speed: 10.0 us/pixel; 12 bits/pixel).

Strain application. Strain (substrate deformation) was applied as described (23, 84), using the computer-controlled vacuum-operated Flex 5000 Jr. Tension System (Flexcell International Corporation). Cells were plated onto collagen-coated silicon membranes and exposed to cyclic biaxial stretch (6% elongation, 0.5 Hz) for indicated times (1, 3, 5 or 7 hours). Control cells were cultured under the same conditions, but no mechanical force was applied. Y-27632 (10 µM), GSK101 (5 nM) or the HC-06 (1 µM) were added to culture media 30 min prior to stretching. Stretch-induced Ca^{2+} influx was studied in cells loaded with Fura-2-AM (5-10 µM) for 60 minutes and stimulated with biaxial stretch (10% elongation, 1 Hz, 15' or 30'). The cells were imaged with an upright Nikon E600FN microscope and a 40x (0.8 N.A. water) objective. 340/380 nm excitation was provided by a Xenon lamp within a Lambda DG4 (Sutter Instruments) wavelength switcher.

Calcium imaging. Pharmacological experiments were conducted in fast-flow chambers (Warner Instruments) on cells loaded with 5-10 µM Fura-2-AM (K_d at RT = 225 nM) for 45 min (23, 128). The saline (pH 7.4) contained (in mM): 98.5 NaCl, 5 KCl, 3 $MgCl_2$, 2 $CaCl_2$, 10 HEPES, 10 D-glucose, 93

mannitol. TRPV4 and Rho reagents were placed into reservoirs connected to a gravity-fed perfusion system (Warner Instruments). Epifluorescence imaging was performed on inverted Nikon microscopes using 40x (1.3 N.A., oil or 0.80 N.A., water) objectives, with excitation for 340 nm and 380 nm filters (Semrock) delivered by a 150W Xenon arc lamp (DG4, Sutter Instruments). Fluorescence emission was high pass-filtered at 510 nm and captured with cooled EMCCD cameras (Photometrics). ΔR/R (peak F_{340}/F_{380} ratio – baseline/baseline) was used to quantify the amplitude of Ca^{2+} signals which were acquired and analyzed using NIS Elements 3.22 software.

Plasmid Constructs and Live Actin Imaging. TM cells were transfected with mApple:actin (0.5 μg/ul) or mCherry:actin (0.5 μg/μl) DNA constructs using Lipofectamine (Invitrogen). Lipofectamine and DNA were diluted separately in Opti-MEM medium; after a quick incubation at RT, the DNA solution was mixed into Lipofectamine solution; the mixture was incubated at RT for about 20 min to obtain the desired N/P ratios. After 24 hour after incubation with the constructs, cells were loaded with Fura-2-AM (5-10 μM) for 45 minutes. TRPV4 and Rho reagents were placed into reservoirs connected to gravity-fed perfusion systems (Warner Instruments). *mApple:actin*/*mCherry:actin* and Fura-2 fluorescence were concurrently imaged with a 40x (1.4 N.A. oil) objective (Nikon Ti, Technical Instruments).

Statistical Analysis. Data are presented as means ± SEM. For histochemistry, ≥10 per experiment were acquired for at least 3 independent experiments. For calcium imaging, ~10-20 cells per slide were averaged, across ~3-6 slides per experiments and 3 independent experiments. Western blot data likewise consists of at least 3 separate experiments. Cell numbers were labeled by "n", while independent experiments were labeled by "N". The statistical comparisons were determined by one-way ANOVA followed by post-hoc Tukey's multiple comparison of means (Origin 8.0, Origin Lab Corporation). $P \leq 0.05$ (*), $P \leq 0.01$ (**), $P \leq 0.001$ (***) and $P \leq 0.0001$ (****) values were considered to be statistically significant.

Results

Stretch-dependent actin stress fiber formation requires TRPV4 activation and Rho signaling

Force-production in non-muscle cells relies on cross-linked actomyosin structures (6, 35). Generally, these are visualized as fluorescently tagged cell-traversing arrays of filamentous actin (F-actin) stress fibers that attach to membrane focal contacts. Physiological levels (6%, 1 hour) of cyclic strain that produce half-maximal $[Ca^{2+}]_{TM}$ responses on the stretch-response curve (23) had no effect on shape or viability of TM cells (Supplementary Fig. 1). Indicating that polymerization of TM F- actin is sensitive to mechanical stress, increased tension was associated with significant increases in stress fiber fluorescence (41.7 ± 4.2%; N = 4; $P < 0.05$) (Fig. 1). The selective TRPV4 blocker HC-067047 (HC-06; 1 µM) did not affect phalloidin signals in resting cells (97.6 ± 4.8%; N = 4) (Fig. 1A & B) but reversed the stress fiber upregulation induced by stretch (to 103.11 ± 4.45%; N = 4; $P < 0.01$) (Fig. 1A & B). Stress fiber fluorescence in non-stretched cells was likewise unaffected by the ROCK inhibitor Y-27632 (10 µM) (88.52 ± 11.65%; N = 4; Fig. 1A & B), whereas ROCK inhibition suppressed the effect of stretch to 71.57 ± 4.81% ($P < 0.01$; N = 4; Fig. 1A & B). TM cell survival was unaffected by the exposure to HC-06 or Y-27632 alone (Supplementary Fig. 1B & C). These observations suggest that *de novo* actin polymerization triggered by mechanical stretch requires activation of TRPV4 and Rho signaling pathways.

-----Figure 1----

Rho/ROCK signaling pathway is downstream from TRPV4

To gain insight into TRPV4 and ROCK mechanisms that underlie stress fiber formation, we conducted ratiometric calcium imaging in the presence of the TRPV4 agonist GSK101 (5 nM) and/or Rho/TRPV4 inhibitors (Fig. 2A-D). GSK101 elevated $\Delta R/R$ to 0.81 ± 0.04 ± 0.27 (n = 164; $P < 0.0001$; Fig. 2A & D), whereas ROCK inhibition had no significant effect on basal $[Ca^{2+}]_i$ (0.13 ± 0.01; n = 66; Fig. 2B & D) or the amplitude of GSK101-induced calcium signals (0.82 ± 0.06; n = 52; Fig. 2C & D). GSK101 similarly facilitated the formation of actin stress fibers in cells transfected with *mCherry:actin* or *mApple:actin* (n = 4, Fig. 2Ai-iii). Concurrent administration of Y-27632 inhibited the activating effect of 5 nM GSK101, resulting in decreased number of stress fibers (n = 4, Fig. 2Ci-iii). In contrast to stress fiber sensitivity to ROCK, $[Ca^{2+}]_i$ elevations induced by 15 or 30 min cyclic stretch (to 0.23 ± 0.02 and

0.22 ± 0.02, respectively; n = 30, N = 4; P < 0.0001) were unaffected by Y-27632 (Fig. 2E & Supplementary Fig. 2), suggesting that Rho-dependent formation of actin stress fibers is downstream from TRPV4. The sensitivity of stretch- and GSK101-induced stress fiber formation to Y-27632 confirms that ROCK is required for actin polymerization driven by both mechanical and chemical inputs.

-----Figure 2----

The small GTPase RhoA is activated by stretch in a TRPV4-dependent manner

We next investigated the stretch-dependence of the small GTPase RhoA, an early responder to tension applied to integrins (36, 37) and a prominent regulator of the TM cytoskeleton (19). One hour of stretch resulted in three-fold increase in RhoA mRNA (3.00 ± 0.72; N = 4; P < 0.05) which was downregulated at longer stretch durations (Fig. 3A). This effect was associated with significant increases in levels of the active (GTP-bound) Rho protein (1.56 ± 0.12; N = 3; P < 0.05) whereas GDP-bound protein levels remained unchanged (Fig. 3B & C). HC-06, but not Y-27632, significantly suppressed stretch-induced upregulation of the active Rho protein (0.99 ± 0.05; P < 0.05; Fig. 3B & C). Hence, tensile strain modulates RhoA transcription and activation in a TRPV4 -dependent manner, but without feedback from ROCK.

-----Figure 3----

Stretch-induced phosphorylation and targeting of Focal Adhesion Kinase (FAK) requires time-dependent TRPV4 activation and Rho signaling

Stress fibers generate force by pulling on adhesion sites, which impose stress on the cytoskeleton via adapter and anchor proteins (10, 38). Mechanical strain facilitates formation of FAs, which are enriched in phosphotyrosinated proteins (39). A particularly important anchoring protein, activated by

mechanically induced integrin clustering (40, 41), is the Focal Adhesion Kinase (FAK). Phosphorylation of FAK was reported to subserves TM stiffness on rigid substrates (42), regulate phagocytosis (43), myocilin-dependent integrin β1 signal transduction (44) but also maintain the structural stability of actin (45). The Protein Tyrosine Kinase 2 (PTK2) gene that encodes FAK was modestly (1.57 ± 0.12-fold) but significantly ($N = 3$; $P < 0.05$) upregulated following 3 hrs strain stimulation and was unaffected at 5 and 7-hour time points (Fig. 4A). We tested whether stretch affects FAK expression and activation by labeling the protein for autophosphorylation at Tyr397 (40, 46). Total FAK protein levels remained constant, but phosphorylation was augmented at 1 and 3 hours to 2.11 ± 0.07; 2.28 ± 0.16 - fold, respectively ($N = 3$-5; $P < 0.01$; Fig. 4B). At 1 hour, Y-27632 suppressed phosphorylation (to 0.88 ± 0.14; $N = 3$; $P < 0.05$) whereas HC-06 had no effect (at 1.87 ± 0.20; $N = 3$) whereas following 3-hours stretch, FAK phosphorylation was inhibited by both TRPV4 and ROCK antagonists (Fig. 4C & D). These data suggest that formation of FAK-containing focal complexes during mechanical stress requires time-dependent ROCK and TRPV4 signaling.

-----Figure 4----

Transient paxillin phosphorylation is an early step in the TM stretch response

FAK shares the submembrane focal space with paxillin, a 64.5 kDa multidomain scaffolding protein that integrates mechanical cues from the ECM with the integrins (47, 48). Stretch does not affect the levels of paxillin mRNA and total protein at any time point ($N = 3$; Fig. 5A, black bars in B & C). However, Western blots showed a striking elevation in activated paxillin (Tyr118 phosphorylation) at 1 hour of stretch, with 2.54 ± 0.27 ($N = 3$; $P < 0.01$) increase (red bars in Fig. 5B). The effect of stretch was blocked by HC-06 (1 µM; 1.18 ± 0.08; $N = 3$; $P < 0.05$) and the calcium chelator BAPTA-AM (100 µM; 0.63 ± 0.06; $N = 3$; $P < 0.01$), but not by Y-27632 (10 µM; $N = 3$; $P = 0.216$) (Fig. 5Di-ii). These data implicate paxillin activation in early, stretch-and time -dependent TM remodeling that requires TRPV4 and Ca^{2+}. Consistent with this, 1 hour stretch caused a remarkable increase in the number of p-paxillin-

immunoreactive (ir) (Tyr31-phosphorylated) puncta (to 1.69 ± 0.11; N = 3; P < 0.05 (Fig. 5E & F and Supplementary Fig. 3) without affecting the number of vinculin-ir puncta (Fig. 5F and Supplementary Fig. 3). However, stretch significantly enhanced the extent of vinculin and p-paxillin colocalizations (from 0.20 ± 0.04 to 0.45 ± 0.10 and from 0.51 ± 0.10 to 0.69 ± 0.07, respectively; N = 3; P < 0.05) in a TRPV4-, BAPTA- and ROCK-dependent manner (Fig. 5G and Supplementary Fig. 3).

-----Figure 5----

Stretch promotes colocalization between vinculin and pFAK

Paxillin is recruited to the actin network via the N-terminal domain of vinculin, a key protein that regulates integrin and anchor protein dynamics that are required for FA enlargement (49). We found that vinculin is recruited to stress fiber-anchored FAs in a force-dependent manner (Fig. 6C, F & G). While mRNA and total vinculin protein expression remained unaffected by stretch (Fig. 6A & B), increased colocalization between vinculin and pFAK was observed at 1 and 3 hours (from 46 ± 3% to 58 ± 3% in 1 hr samples and from 57 ± 2% to 71 ± 2% in 3 hr samples; P < 0.05; N = 3) (Fig. 6F & G). This effect was sensitive to Y-27632 at 1 hour (to 39.39 ± 5.04%; P < 0.05; N = 3) and HC-06 at 3 hours (54 ± 4%; P < 0.05; N = 3; Fig. 6F & G). In resting cells, vinculin colocalized with pFAK at the edges of stress fibers (Fig. 6C), with the number of pFAK-ir FA clusters increasing at 1 and 3 hour stretch (by 65.79 ± 20.22% and 34.54 ± 1.01%; P < 0.01 and 0.001, respectively; N = 3; Fig. 6D & E). The increase in immunoreactive puncta was associated with a modest but significant, increase in pFAK - vinculin colocalization (from 76.03 ± 2.36% to 85.44 ± 1.25% and from 74.12 ± 1.12 to 86.65 ± 3.1%, respectively; P < 0.05; N = 3) (Fig. 6F & G). Y-27632, but not HC-06, inhibited pFAK upregulation and its interaction with vinculin at 1 hour, whereas HC-06 and Y-27632 both suppressed the effect after 3 hours of stretch (Fig. 6C-G). These findings confirm the Rho-dependence of FAK activation (50) and suggest that TRPV4-dependent stabilization of FAK-vinculin-containing FAs involves time-dependent Rho signaling.

----Figure 6---

Stretch also increases in vinculin-ir (1.27 ± 0.05; P < 0.01; N = 3) and FA size that were antagonized by ROCK and TRPV4 blockers to 1.01 ± 0.03 and 1.05 ± 0.08, respectively (P < 0.05; N = 3) (Fig. 7A, B and Supplementary Fig. 4A). We tested for stretch-dependence of vinculin activation by labeling for Tyr1065, which is important for force generation (51). A significant increase in activated vinculin (1.78 ± 0.25; P < 0.05; N = 3) was observed following 1 hour of stretch, an effect that was suppressed by Y-27632 (0.75 ± 0.1; P < 0.05; N = 3) and HC-06 (0.99 ± 0.25; P < 0.05; N = 3) (Fig. 7C, D and Supplementary Fig. 4B). Thus, stretch-induced vinculin activation requires Rho and TRPV4 signaling.

----Figure 7---

Stretch-induced translocation of zyxin from FAs to polymerized actin requires TRPV4 and calcium

The FA protein zyxin mediates force-dependent interactions between actin regulatory proteins and actin (52, 53) and is sensitive to TGFβ2, a glaucoma-promoting cytokine known to drive TM actin polymerization (54, 55). Assessment of zyxin mRNA and protein levels after 1 - 7 hours exposure to cyclic strain showed significant upregulation in transcription following 1 hour (2.35 ± 0.19-fold) and 5 hours (2.43 ± 0.22-fold) of stretch (N = 3-4; P □ 0.01; Fig. 8A & B), whereas total zyxin protein levels were unaffected for up to 7 hours (2.55 ± 0.16; N = 3; P □ 0.05) (Fig. 8B & C). As with other FA adhesome components (Fig. 4 & 5), stretch augmented zyxin phosphorylation (at S142/143) by 2.45 ± 0.48 and 2.69 ± 0.48- fold following 1- and 3-hour stretch, respectively (N = 3-4; P □ 0.05 and 0.01; Fig. 8B & C). Zyxin phosphorylation at 1 hour was unaffected by Y-27632, HC-06 or BAPTA (Fig. 8C, D & Ei-ii) whereas TRPV4 and ROCK blockade significantly reduced the levels of phosphorylated-zyxin at 3 hours stretch (1.18 ± 0.31 and 1.32 ± 0.29, respectively; N = 3-4; P □ 0.05) (Fig. 8C & D). In unstimulated cells, zyxin-ir was largely confined to FA sites whereas stretch induced a remarkable

translocation towards actin stress fibers (Fig. 9 and Supplementary Fig. 5), an effect that was sensitive to HC-06 and Y-27632. Zyxin translocation induced by strain was presumably associated with increased cytoskeletal tension and contractility (56-58).

----Figures 8 and 9---

Discussion

Our study identifies the molecular mechanism through which physiological strains regulate the architecture and function of trabecular meshwork cells. We employed strains that mirrored *in situ* biomechanical stress on corneoscleral beams and juxtacanalicular lamellae (~10% –20% strain for pressure differentials of ~5 – 15 mm Hg) (59-61), and a stretch cycle (1 Hz) that reflected ocular pulse dynamics (e.g., 62, 63), to discover that cyclic strains induce cytoskeletal and FA remodeling through obligatory activation of TRPV4 channels, Rho signaling, and TRPV4-Rho interactions. We conclude that TRPV4 functions as the likely SAC transducer of TM stretch response that underpins myofibroblast transdifferentiation, shown previously as stretch- and IOP-dependent increases in F-actin, tyrosine phosphorylation, αSMA & Rho-ROCK signaling and TGFβ release that underlie the stiffening of TM cells (15, 18, 62, 64-69). Given that strain represents a principal aspect of IOP-generated mechanical force that shapes trabecular outflow (61) whereas cytoskeletal remodeling constitutes the central aspect of glaucomatous TM remodeling (19), elucidation of TM mechanotransduction and Rho signaling pathways brings insight into the biology of the ocular outflow system and identifies pathways that can be targeted to reverse cytoskeletal impairments in glaucoma.

Our results establish a mechanistic framework for howTRPV4 antagonists, actin disruptors and ROCK inhibitors suppress TM stiffness, ECM release and IOP in hypertensive eyes (21-23, 69, 70, 72, 73) by adding two important insights: First, Rho signals are downstream from TRPV4, with TRPV4 mechanotransduction and ROCK activation both necessary and sufficient for increased F-actin

polymerization induced by cyclic mechanical strain. This provides the molecular mechanotransduction context for increased contractility in mechanically stressed TM cells (11, 68). The obliteration of stretch-evoked increases in stress fiber fluorescence by the cell-permeable pyridine derivative Y-27632 (Fig. 1 & 2) is consistent with ROCK functioning as the master regulator of actin polymerization, contractility and remodeling in mechanically stressed TM (22, 70). Rao's group found that stretch elevates the TM levels of activated RhoA, phosphorylated paxillin and MLCK through a process that mirrors aberrant Rho/ROCK activation and fibrogenic activity during the epithelial-to-mesenchymal transition (EMT). Rho-dependent stress fiber formation, myosin II phosphorylation, and increased expression of αSMA, TGFβ2 and ECM proteins have been correlated with reduced outflow facility in mouse eyes (19, 68, 71). Here, we link the EMT induced by mechanical stress (19) to dynamic, TRPV4 and ROCK-dependent upregulation of integrin-ECM contacts within the FAs. Indicating that the SAC and the cytoskeletal regulator together control strain-dependent formation, maturation and maintenance of FAs, TRPV4 and ROCK blockers reduced the number and size of activated FAs, and suppressed colocalization between key components of the FA complex (p-paxillin and vinculin, pFAK and vinculin; Fig. 5, 6 & 7). Collectively, these findings suggest a mechanoreciprocity mechanism that reinforces TM cytoarchitecture in the presence of chronic strains by promoting the transition towards the contractile myofibroblast.

Membrane stretch promotes F-actin and αSMA expression, MLCK phosphorylation and biosynthesis of ECM that inhibit aqueous outflow (19, 68, 74). Indicating that TRPV4 functions as the SAC that mediates stretch-induced cytoskeletal stiffening, GSK101 mirrored the effect of stretch on stress fiber formation whereas HC-06 blocks stretch-induced F-actin upregulation. ROCK inhibition downregulated pMLCK and αSMA and suppressed F-actin polymerization (62, 68, 71) whereas the absence of Y-27632 effects on TRPV4-induced $[Ca^{2+}]_i$ signals (Fig. 2) rules out a major role for cytosolic or membrane Rho signaling (75) in TRPV4 channel gating, translocation and/or expression and places ROCK signaling downstream from TRPV4. Consistent with this conclusion, the effects of cyclic stretch on cytoskeletal remodeling and myofibroblast transformation can be substituted through constitutive

activation of the Rho pathway (68, 76, 77) or TRPV4 overactivation (31, 34, 78). To the best of our knowledge, our study is among the first to systematically examine the convergence of the two pathways at the level of multiple constituents of the tensile transduction mechanism.

In general, SAC gating is influenced by the properties of the lipid bilayer and by channel interactions with the cytoskeleton and the ECM. The obligatory involvement of TRPV4 in force-induced stress fiber formation, FA reinforcement and fibrosis accords with its functions as a transducer of pressure (24, 79), ECM stiffness (80), cell swelling (81-84), shear stress (85, 86), and its roles in gene expression, integrin signaling (87), tensile activation of vinculin (88) and fibrotic remodeling (34). In contrast to Piezo1 and TREK1 channels which are directly activated by pressure/stretch/indentation (89, 90), the biophysical mechanism that activates TRPV4 channels in the presence of strain is not understood (81, 84, 91-93, 79, 80, 93, 95). It might involve β1 integrins, which bind the channel (5, 30, 87), are expressed in human and mouse TM (97, 98), interact with ROCK (75), and contribute to IOP regulation and glaucoma (99, 100). Interestingly, pretreatment with FAK or β1 integrin inhibitors suppressed sensitization of TRPV4 channels by mechanical stressors (Baratchi et al., 2017). Another clue is TRPV4 activation by arachidonic acid, which is produced in response to stretch and might enhance TM sensitivity to weak hydrodynamic loading (23, 93, 96).

Our data identify TRPV4 -mechanotransduction as a venue for Ca^{2+} influx that is necessary and sufficient for stretch-induced reinforcement of stress fibers and growth of focal adhesions. Ca^{2+} activates multiple FA-associated proteins, including vinculin (Gilchrist et al., 2019), Src family kinases (SFKs), talin (Kerstein et al., 2013) and MLC/Rho-Rho kinase pathways (Sakurada et al., 2003). ~30% of $[Ca^{2+}]_{TM}$ signal induced by TRPV4 activation is subserved by secondary store release (23), and it is likely that the effects of stretch on cytoskeletal and FA remodeling observed in the present work include auxiliary contributions from Ca^{2+} stores and/or store-operated channels (Abad et al., 2008). Agents that induce Ca^{2+} release from intracellular stores similarly stimulate TM contractility and TGFβ1 signaling to augment the trabecular outflow resistance (76, 101-103).

Our data demonstrate that mechanical stress has dramatic repercussions for the activation state, expression and localization of focal adaptor proteins. This process requires TRPV4 and calcium, as indicated by suppression of stretch-evoked increases in activated RhoA GTPase, paxillin (Tyr118), vinculin (Tyr1065) and zyxin (S142/143) phosphorylation (Figs. 3, 5, 7 & 9) by HC-06 and/or BAPTA-AM. The large early increases in paxillin phosphorylation, its sensitivity to local Ca^{2+} elevations and its localization to FAs point at paxillin as initial targets of increased strain. Consistent with this, TRPV4 inhibition and chelation of calcium suppressed stretch-dependent upregulation in p-paxillin expression, number of p-paxillin-ir sites and the increase in p-paxillin/pFAK-vinculin colocalization. The absence of effect at the transcript level suggests that, within the time-frame of our experiments (1 – 3 hours), strain principally regulates FA remodeling through post-translational modifications. Similar to other focal anchoring proteins, paxillin activation was sensitive to TRPV4-mediated Ca^{2+} influx and ROCK, most likely via Rho-dependent "inside-out" changes in integrin affinity (107). FAK migration to vinculin-containing sites and phosphorylation of zyxin acquired TRPV4-dependence after three hours of stretch, suggesting involvement of additional Ca^{2+}-dependent steps that regulate stress fiber enlargement, FA maturation and translocation of zyxin complexes into F-actin stress fibers. The mechanisms that mediate these processes remain to be investigated in the future, but may include the Ca^{2+}- calmodulin kinase II (CaMKII) which binds integrins upon increases in $[Ca^{2+}]_i$ (108, 109), prolongs the activation of RhoA (110) and regulates the tensile force in SMCs and myofibroblasts (111), stretch-sensitive Src family tyrosine kinases which bind TRPV4 and integrins, and the protein kinase C, which regulates TGFβ1-dependent upregulation in F-actin and TM contractility (11, 76, 115).

A key question in glaucoma research concerns the molecular mechanisms through which elevations in IOP augment the TM resistance to aqueous outflow (61). Previous investigations tended to study the effects of stretch after >8 hours-to-days of stimulation (65, 116-119) however, we find that many key elements of force-induced TM remodeling and contractility are in place at 1-3 hours of stretch. These include stress fiber upregulation, phosphorylation of RhoA, paxillin, FAK and zyxin, and translocation of FA components (zyxin) (Figs. 2-9) to reinforce stress fibers, augment FA assembly and

promote cell contractility. Because mature FAs contain myosin II they directly participate in the contractile response. Hence, TM plasticity may be more dynamic than anticipated, involving cooperation between different compartments to compensate for the increased mechanical stress.

Our findings are consistent with a model whereby TM cells rely on TRPV4 polymodality, Rho GTPases, integrins and Ca^{2+} to integrate parallel aspects of the mechanical and signaling milieu in the anterior eye. These mechanisms may be homeostatic at short time scales as IOP fluctuates in response to ocular pulse, eye rubbing, saccades, blinking, swim goggles and yoga poses (61, 63) but become pathological in the presence of sustained stress when TM cells undergo myofibroblast transdifferentiation epitomized by TRPV4-dependent cytoskeletal stiffening, strengthened membrane-ECM contacts and increased contractility. Similar functions were ascribed to TRPV4 in SMC, endothelial, epithelial and mesenchymal remodeling during fibroproliferative cancer, lung and heart diseases (31, 33, 34, 120, 121), potentially suggesting a universal program of tissue fibrosis and/or repair. TRPV4 localization to retinal ganglion cells, microglia, Müller cells and endothelial cells (32, 69, 124, 125), elevated Rho GTPase levels in the glaucomatous optic nerve head of (122) and improved ganglion cell survival following ROCK inhibitor treatment (123) suggest that TRPV4-Rho interactions may also occur in the hypertensive posterior eye. In contrast to Y-2763, which triggers wholesale dissolution of F-actin (Fig. 2), TRPV4 antagonists have no observable side effects (23) and may be used to target the mechanotransducer to maintain function while preserving the cells' capacity for actomyosin regulation. Because the Rho pathway is downstream of TRPV4, targeting the channel could be a viable strategy that combines IOP-lowering with neuroprotection.

Acknowledgements

We thank Dr. Mary Beckerle (University of Utah) for actin and zyxin reagents, and helpful discussions and for Dr. Amy Lin (University of Utah, Moran Eye Center) for the human donor tissues.

References

1. Eyckmans, J., Boudou, T., Yu, X., Chen, C.S. (2011) A hitchhiker's guide to mechanobiology. *Dev Cell.* 21, 35-47.
2. Katta, S., Krieg, M., Goodman, M.B. (2015) Feeling force: physical and physiological principles enabling sensory mechanotransduction. *Annu Rev Cell Dev Biol.* 31, 347-71.
3. Grosheva, I., Vittitow, J.L., Goichberg, P., Gabelt, B.T., Kaufman, P.L., Borrás, T., Geiger, B., Bershadsky, A.D. (2006) Caldesmon effects on the actin cytoskeleton and cell adhesion in cultured HTM cells. *Exp Eye Res.* 82, 945-58.
4. Tsai, I.J., Chou, C.H., Yang, Y.H., Lin, W.C., Lin, Y.H., Chow, L.P., Lee, H.H., Kao, P.G., Liau, W.T., Jou, T.S., Tsau, Y.K. (2015) Inhibition of Rho-associated kinase relieves C5a-induced proteinuria in murine nephrotic syndrome. *Cell Mol Life Sci.* 72, 3157-71.
5. Arora, P.D., Di Gregorio, M., He, P., McCulloch, C.A. (2017) TRPV4 mediates the Ca^{2+} influx required for the interaction between flightless-1 and non-muscle myosin, and collagen remodeling. *J Cell Sci.* 130, 2196-2208.
6. Livne, A., Geiger, B. (2016) The inner workings of stress fibers□-□from contractile machinery to focal adhesions and back. *J Cell Sci.* 129, 1293-304.
7. Kanchanawong, P., Shtengel, G., Pasapera, A.M., Ramko, E.B., Davidson, M.W., Hess, H.F., Waterman, C.M. (2010) Nanoscale architecture of integrin-based cell adhesions. *Nature.* 468, 580-4.
8. Arias-Salgado, E.G., Lizano, S., Sarkar, S., Brugge, J.S., Ginsberg, M.H., Shattil, S.J. (2003) Src kinase activation by direct interaction with the integrin beta cytoplasmic domain. *Proc Natl Acad Sci U S A.* 100, 13298-302.
9. Sun, Z., Guo, S.S., Fässler, R. (2016) Integrin-mediated mechanotransduction. *J Cell Biol.* 215, 445-456.
10. Burridge, K. (2017) Focal adhesions: a personal perspective on a half century of progress. *FEBS J.* 284, 3355-3361.
11. Wiederholt, M., Thieme, H., Stumpff, F. (2000) The regulation of trabecular meshwork and ciliary muscle contractility. *Prog Retin Eye Res.* 19, 271-95.

12. Johnstone, M.A. (2004) The aqueous outflow system as a mechanical pump: evidence from examination of tissue and aqueous movement in human and non-human primates. *J Glaucoma*. 13, 421-38.

13. Gong, H., Freddo, T.F. (2009) The washout phenomenon in aqueous outflow--why does it matter? *Exp Eye Res.* 88, 729-37.

14. Overby, D.R., Bertrand, J., Schicht, M., Paulsen, F., Stamer, W.D., Lütjen-Drecoll, E. (2014) The structure of the trabecular meshwork, its connections to the ciliary muscle, and the effect of pilocarpine on outflow facility in mice. *Invest Ophthalmol Vis Sci.* 55, 3727-36.

15. Welge-Lüssen, U., May, C.A., Eichhorn, M., Bloemendal, H., Lütjen-Drecoll. E. (1999) AlphaB-crystallin in the trabecular meshwork is inducible by transforming growth factor-beta. *Invest Ophthalmol Vis Sci.* 40, 2235-41.

16. Raghunathan, V.K., Benoit, J., Kasetti, R., Zode, G., Salemi, M., Phinney, B.S., Keller, K.E., Staverosky, J.A., Murphy, C.J., Acott, T., Vranka, J. (2018) Glaucomatous cell derived matrices differentially modulate non-glaucomatous trabecular meshwork cellular behavior. *Acta Biomater.* 71, 444-459.

17. Li, G., Lee, C., Agrahari, V., Wang, K., Navarro, I., Sherwood, J.M., Crews, K., Farsiu, S., Gonzalez, P., Lin, C.W., Mitra, A.K., Ethier, C.R., Stamer, W.D. (2019) In vivo measurement of trabecular meshwork stiffness in a corticosteroid-induced ocular hypertensive mouse model. *Proc Natl Acad Sci U S A.* 116, 1714-1722.

18. Last, J.A., Pan, T., Ding, Y., Reilly, C.M., Keller, K., Acott, T.S., Fautsch, M.P., Murphy, C.J., Russell, P. (2011) Elastic modulus determination of normal and glaucomatous human trabecular meshwork. *Invest Ophthalmol Vis Sci.* 52, 2147-52.

19. Pattabiraman, P.P., Inoue, T., Rao, P.V. (2015) Elevated intraocular pressure induces Rho GTPase mediated contractile signaling in the trabecular meshwork. *Exp Eye Res.* 136, 29-33.

20. Vahabikashi, A., Gelman, A., Dong, B., Gong, L., Cha. E.D.K., Schimmel, M., Tamm, E.R., Perkumas, K., Stamer, W.D., Sun, C., Zhang, H.F., Gong, H., Johnson, M. (2019) Increased stiffness and flow resistance of the inner wall of Schlemm's canal in glaucomatous human eyes. *Proc Natl Acad Sci U S A.* pii: 201911837. doi: 10.1073/pnas.1911837116.

21. Peterson, J.A., Tian, B., McLaren, J.W., Hubbard, W.C., Geiger, B., Kaufman, P.L. (2000) Latrunculins' effects on intraocular pressure, aqueous humor flow, and corneal endothelium. *Invest Ophthalmol Vis Sci.* 41, 1749-58.

22. Rao, P.V., Pattabiraman, P.P., Kopczynski, C. (2017) Role of the Rho GTPase/Rho kinase signaling pathway in pathogenesis and treatment of glaucoma: Bench to bedside research. *Exp Eye Res.* 158, 23-32.

23. Ryskamp, D.A., Frye, A.M., Phuong, T.T., Yarishkin, O., Jo, A.O., Xu, Y., Lakk, M., Iuso, A., Redmon, S.N., Ambati, B., Hageman, G., Prestwich, G.D., Torrejon, K.Y., Križaj, D. (2016) TRPV4 regulates calcium homeostasis, cytoskeletal remodeling, conventional outflow and intraocular pressure in the mammalian eye. *Sci Rep.* 6, 30583.

24. Yarishkin, O., Phuong, T.T.T., Križaj, D. (2019) Trabecular Meshwork TREK-1 Channels Function as Polymodal Integrators of Pressure and pH. *Invest Ophthalmol Vis Sci.* 60, 2294-2303.

25. Križaj, D. (2020) No cell is an island: trabecular meshwork ion channels as sensors of the ambient milieu. In: Glaucoma Research and Clinical Advances Vol. 3, Eds. John R. Samples & Paul A. Knepper, Kugler Publications Amsterdam

26. Luo, N., Conwell, M.D., Chen, X., Kettenhofen, C.I., Westlake, C.J., Cantor, L.B., Wells, C.D., Weinreb, R.N., Corson, T.W., Spandau, D.F., Joos, K.M., Iomini, C., Obukhov, A.G., Sun, Y. (2014) Primary cilia signaling mediates intraocular pressure sensation. *Proc Natl Acad Sci U S A.* 111, 12871-6.

27. Ramadass, R., Becker, D., Jendrach, M., Bereiter-Hahn, J. (2007) Spectrally and spatially resolved fluorescence lifetime imaging in living cells: TRPV4-microfilament interactions. *Arch Biochem Biophys.* 463, 27-36.

28. Kida, N., Sokabe, T., Kashio, M., Haruna, K., Mizuno, Y., Suga, Y., Nishikawa, K., Kanamaru, A., Hongo, M., Oba, A., Tominaga, M. (2012) Importance of transient receptor potential vanilloid 4 (TRPV4) in epidermal barrier function in human skin keratinocytes. *Pflugers Arch.* 463, 715-25.

29. Sokabe, T., Fukumi-Tominaga, T., Yonemura, S., Mizuno, A., Tominaga, M. (2010) The TRPV4 channel contributes to intercellular junction formation in keratinocytes. *J Biol Chem.* 285, 18749-58.

30. Potla, R., Hirano-Kobayashi, M., Wu, H., Chen, H., Mammoto, A., Matthews, B.D., Ingber, D.E. (2019) Molecular mapping of transmembrane mechanotransduction through the β1 integrin-CD98hc-TRPV4 axis. bioRxiv doi: https://doi.org/10.1101/617092

31. Rahaman, S.O., Grove, L.M., Paruchuri, S., Southern, B.D., Abraham, S., Niese, K.A., Scheraga, R.G., Ghosh, S., Thodeti, C.K., Zhang, D.X., Moran, M.M., Schilling, W.P., Tschumperlin, D.J., Olman, M.A. (2014) TRPV4 mediates myofibroblast differentiation and pulmonary fibrosis in mice. *J Clin Invest.* 124, 5225-38.

32. Phuong, T.T.T., Redmon, S.N., Yarishkin, O., Winter, J.M., Li, D.Y., Križaj, D. (2017) Calcium influx through TRPV4 channels modulates the adherens contacts between retinal microvascular endothelial cells. *J Physiol.* 595, 6869-6885.

33. Nam, S., Gupta, V.K., Lee, H.P., Lee, J.Y., Wisdom, K.M., Varma, S., Flaum, E.M., Davis, C., West, R.B., Chaudhuri, O. (2019) Cell cycle progression in confining microenvironments is regulated by a growth-responsive TRPV4-PI3K/Akt-p27^{Kip1} signaling axis. *Sci Adv.* 5, eaaw6171.

34. Grove, L.M., Mohan, M.L., Abraham, S., Scheraga, R.G., Southern, B.D., Crish, J.F., Naga, Prasad, S.V., Olman, M.A. (2019) Translocation of TRPV4-PI3Kγ complexes to the plasma membrane drives myofibroblast transdifferentiation. *Sci Signal.* 12(607).

35. Hotulainen, P., Lappalainen, P. (2006) Stress fibers are generated by two distinct actin assembly mechanisms in motile cells. *J Cell Biol.* 173, 383-94.

36. Burridge, K., Wennerberg, K. (2004) Rho and Rac take center stage. *Cell.* 116, 167-79.

37. Guilluy, C., Dubash, A.D., García-Mata, R. (2011) Analysis of RhoA and Rho GEF activity in whole cells and the cell nucleus. *Nat Protoc.* 6, 2050-60.

38. Soine´, J.R., Brand, C.A., Stricker, J., Oakes, P.W., Gardel, M.L., and Schwarz, U.S. (2015) Model-based traction force microscopy reveals differential tension in cellular actin bundles. *PLoS Comput. Biol.* 11, e1004076.

39. Geiger, B., Bershadsky, A., Pankov, R., Yamada, K.M. (2001) Transmembrane crosstalk between the extracellular matrix--cytoskeleton crosstalk. *Nat Rev Mol Cell Biol.* 2, 793-805.

40. Calalb, M.B., Polte, T.R., Hanks, S.K. (1995) Tyrosine phosphorylation of focal adhesion kinase at sites in the catalytic domain regulates kinase activity: a role for Src family kinases. *Mol Cell Biol.* 15, 954-63.

41. Seong, J., Tajik, A., Sun, J., Guan, J.L., Humphries, M.J., Craig, S.E., Shekaran, A., García, A.J., Lu, S., Lin, M.Z., Wang, N., Wang, Y. (2013) Distinct biophysical mechanisms of focal adhesion kinase mechanoactivation by different extracellular matrix proteins. *Proc Natl Acad Sci U S A.* 110, 19372-7.

42. Schlunck, G., Han, H., Wecker, T., Kampik, D., Meyer-ter-Vehn, T., Grehn, F. (2008) Substrate rigidity modulates cell matrix interactions and protein expression in human trabecular meshwork cells. *Invest Ophthalmol Vis Sci.* 49, 262-9.

43. Gagen, D., Filla, M.S., Clark, R., Liton, P., Peters, D.M. (2013) Activated αvβ3 integrin regulates αvβ5 integrin-mediated phagocytosis in trabecular meshwork cells. *Invest Ophthalmol Vis Sci.* 54, 5000-11.

44. Kwon, H.S., Tomarev, S.I. (2011) Myocilin, a glaucoma-associated protein, promotes cell migration through activation of integrin-focal adhesion kinase-serine/threonine kinase signaling pathway. *J Cell Physiol.* 226, 3392-402.

45. O'Brien, E.T., Kinch, M., Harding, T.W., Epstein, D.L. (1997) A mechanism for trabecular meshwork cell retraction: ethacrynic acid initiates the dephosphorylation of focal adhesion proteins. *Exp Eye Res.* 65, 471-83.

46. Schaller, M.D., Hildebrand, J.D., Shannon, J.D., Fox, J.W., Vines, R.R., Parsons, J.T. (1994) Autophosphorylation of the focal adhesion kinase, pp125FAK, directs SH2-dependent binding of pp60src. *Mol Cell Biol.* 14, 1680-8.

47. Zhou, L., Cheng, E.L., Rege, P., Yue, B.Y. (2000) Signal transduction mediated by adhesion of human trabecular meshwork cells to extracellular matrix. *Exp Eye Res.* 70, 457-65.

48. Zaidel-Bar, R., Geiger, B. (2010) The switchable integrin adhesome. *J Cell Sci.* 123, 1385-8.

49. Giannone, G. (2015) Super-resolution links vinculin localization to function in focal adhesions. *Nat Cell Biol.* 17, 845-7.

50. Sinnett-Smith, J., Lunn, J.A., Leopoldt, D., Rozengurt, E. (2001) Y-27632, an inhibitor of Rho-associated kinases, prevents tyrosine phosphorylation of focal adhesion kinase and paxillin induced by bombesin: dissociation from tyrosine phosphorylation of p130(CAS). *Exp Cell Res.* 266, 292-302.

51. Auernheimer, V., Lautscham, L.A., Leidenberger, M., Friedrich, O., Kappes, B., Fabry, B., Goldmann, W.H. (2015) Vinculin phosphorylation at residues Y100 and Y1065 is required for cellular force transmission. *J Cell Sci.* 128, 3435-43.

52. Yi, J., Kloeker, S., Jensen, C.C., Bockholt, S., Honda, H., Hirai, H., Beckerle, M.C. (2002) Members of the Zyxin family of LIM proteins interact with members of the p130Cas family of signal transducers. *J Biol Chem.* 277, 9580-9.

53. Hoffman, L.M., Jensen, C.C., Chaturvedi, A., Yoshigi, M., Beckerle, M.C. (2012) Stretch-induced actin remodeling requires targeting of zyxin to stress fibers and recruitment of actin regulators. *Mol Biol Cell. 23*, 1846-59.

54. Bollinger, K.E., Crabb, J.S., Yuan, X., Putliwala, T., Clark, A.F., Crabb, J.W. (2011) Quantitative proteomics: TGFβ signaling in trabecular meshwork cells. *Invest Ophthalmol Vis Sci.* 52, 8287-94.

55. Montecchi-Palmer, M., Bermudez, J.Y., Webber, H.C., Patel, G.C., Clark, A.F, Mao, W. (2017) TGFβ2 Induces the Formation of Cross-Linked Actin Networks (CLANs) in Human Trabecular Meshwork Cells Through the Smad and Non-Smad Dependent Pathways. *Invest Ophthalmol Vis Sci.* 58, 1288-1295.

56. Yoshigi, M., Hoffman, L.M., Jensen, C.C., Yost, H.J., Beckerle, M.C. (2005) Mechanical force mobilizes zyxin from focal adhesions to actin filaments and regulates cytoskeletal reinforcement. *J Cell Biol.* 171, 209-15.

57. Ngu, H., Feng, Y., Lu, L., Oswald, S.J., Longmore, G.D., Yin, F.C. (2010) Effect of focal adhesion proteins on endothelial cell adhesion, motility and orientation response to cyclic strain. *Ann Biomed Eng.* 8, 208-22.

58. Fabry, B., Klemm, A.H., Kienle, S., Schäffer, T.E., Goldmann, W.H. (2011) Focal adhesion kinase stabilizes the cytoskeleton. *Biophys J.* 101, 2131-8.

59. Grierson, I., Lee, W,R. (1975) The fine structure of the trabecular meshwork at graded levels of intraocular pressure. (2) Pressures outside the physiological range (0 and 50 mmHg). *Exp Eye Res.* 20, 523-30.

60. Downs, J.C., Burgoyne, C.F., Seigfreid, W.P., Reynaud, J.F., Strouthidis, N.G., Sallee, V. (2011) 24-hour IOP telemetry in the nonhuman primate: implant system performance and initial characterization of IOP at multiple timescales. *Invest Ophthalmol Vis Sci.* 52, 7365-75.

61. Sherwood, J.M., Stamer, W.D., Overby, D.R. (2019) A model of the oscillatory mechanical forces in the conventional outflow pathway. *J R Soc Interface.* 16, 20180652.

62. Ramos, R.F., Sumida, G.M., Stamer, W.D. (2009) Cyclic mechanical stress and trabecular meshwork cell contractility. *Invest Ophthalmol Vis Sci.* 50, 3826-32.

63. Turner, D.C., Edmiston, A.M., Zohner, Y.E., Byrne, K.J., Seigfreid, W.P., Girkin, C.A., Morris, J.S., Downs, J.C. (2019) Transient Intraocular Pressure Fluctuations: Source, Magnitude, Frequency, and Associated Mechanical Energy. *Invest Ophthalmol Vis Sci.* 60, 2572-2582.

64. Tamm, E.R., Siegner, A., Baur, A., Lütjen-Drecoll, E. (1996) Transforming growth factor-beta 1 induces alpha-smooth muscle-actin expression in cultured human and monkey trabecular meshwork. *Exp Eye Res.* 62, 389-97.

65. Tumminia, S.J., Mitton, K.P., Arora, J., Zelenka, P., Epstein, D.L., Russell, P. (1998) Mechanical stretch alters the actin cytoskeletal network and signal transduction in human trabecular meshwork cells. *Invest Ophthalmol Vis Sci.* 39, 1361-71.

66. Ramos, R.F., Stamer, W.D. (2008) Effects of cyclic intraocular pressure on conventional outflow facility. *Invest Ophthalmol Vis Sci.* 49, 275-81.

67. WuDunn, D. (2009) Mechanobiology of trabecular meshwork cells. *Exp Eye Res.* 88, 718-23.

68. Pattabiraman, P.P., Rao, P.V. (2010) Mechanistic basis of Rho GTPase-induced extracellular matrix synthesis in trabecular meshwork cells. *Am J Physiol Cell Physiol.* 298, C749-63.

69. Križaj, D. (2019) What is glaucoma? *Webvision: The Organization of the Retina and Visual System [Internet]*. University of Utah Health Sciences Center, Salt Lake City, UT

70. Honjo, M., Tanihara, H., Inatani, M., Kido, N., Sawamura, T., Yue, B.Y., Narumiya, S., Honda, Y. (2001) Effects of rho-associated protein kinase inhibitor Y-27632 on intraocular pressure and outflow facility. *Invest Ophthalmol Vis Sci.* 42, 137-44.

71. Pattabiraman, P.P., Maddala, R., Rao, P.V. (2014) Regulation of plasticity and fibrogenic activity of trabecular meshwork cells by Rho GTPase signaling. *J Cell Physiol*. 229, 927-42.

72. Epstein, D.L., Rowlette, L.L., Roberts, B.C. (1999) Acto-myosin drug effects and aqueous outflow function. *Invest Ophthalmol Vis Sci*. 40, 74-81.

73. Ethier, C.R., Read, A.T., Chan, D.W. (2006) Effects of latrunculin-B on outflow facility and trabecular meshwork structure in human eyes. *Invest Ophthalmol Vis Sci*. 47, 1991-8.

74. Vittitow, J.L., Garg, R., Rowlette, L.L., Epstein, D.L., O'Brien, E.T., Borrás, T. (2002) Gene transfer of dominant-negative RhoA increases outflow facility in perfused human anterior segment cultures. *Mol Vis*. 8, 32-44.

75. Wakabayashi, S., Morihara, H., Yokoe, S., Nakagawa, T., Moriwaki, K., Tomoda, K., Asahi, M. (2019) Overexpression of Na^+/H^+ exchanger 1 specifically induces cell death in human iPS cells via sustained activation of the Rho kinase ROCK. *J Biol Chem.* 294, 19577-19588.

76. Nakamura, Y., Hirano, S., Suzuki, K., Seki, K., Sagara, T., Nishida, T. (2002) Signaling mechanism of TGF-beta1-induced collagen contraction mediated by bovine trabecular meshwork cells. *Invest Ophthalmol Vis Sci*. 43, 3465-72.

77. Junglas, B., Kuesper, S., Seleem, A.A., Struller, T., Ullmann, S., Bösl, M., Bosserhoff, A., Köstler, J., Wagner, R., Tamm, E.R., Fuchshofer, R. (2012) Connective tissue growth factor causes glaucoma by modifying the actin cytoskeleton of the trabecular meshwork. *Am J Pathol.* 180, 2386-403.

78. LeBleu, V.S., Taduri, G., O'Connell, J., Teng, Y., Cooke, V.G., Woda, C., Sugimoto, H., Kalluri, R. (2013) Origin and function of myofibroblasts in kidney fibrosis. *Nat Med.* 19, 1047-53.

79. Loukin, S., Zhou, X., Su, Z., Saimi, Y., Kung, C. (2010) Wild-type and brachyolmia-causing mutant TRPV4 channels respond directly to stretch force. *J Biol Chem.* 285, 27176-81.

80. Servin-Vences, M.R., Moroni, M., Lewin, G.R., Poole, K. (2017) Direct measurement of TRPV4 and PIEZO1 activity reveals multiple mechanotransduction pathways in chondrocytes. *Elife.* 6, pii: e21074.

81. Strotmann, R., Harteneck, C., Nunnenmacher, K., Schultz, G., Plant, T.D. (2000) OTRPC4, a nonselective cation channel that confers sensitivity to extracellular osmolarity. *Nat Cell Biol.* 2, 695-702.

82. Jo, A.O., Lakk, M., Frye, A.M., Phuong, T.T., Redmon, S.N., Roberts, R., Berkowitz, B.A., Yarishkin, O., Križaj, D. (2016) Differential volume regulation and calcium signaling in two ciliary body cell types is subserved by TRPV4 channels. *Proc Natl Acad Sci U S A.* 113, 3885-90.

83. Toft-Bertelsen, T.L., Križaj, D., MacAulay, N. (2017) When size matters: transient receptor potential vanilloid 4 channel as a volume-sensor rather than an osmo-sensor. *J Physiol.* 595, 3287-3302.

84. Lapajne, L., Lakk, M., Yarishkin, O., Gubeljak, L., Hawlina, M., Križaj, D. (2020) Polymodal sensory transduction in mouse corneal epithelial cells. *Invest Ophthalmol Vis Sci.* 61, 1-14.

85. Köhler, R., Hoyer, J. (2007) Role of TRPV4 in the Mechanotransduction of Shear Stress in Endothelial Cells. In: *TRP Ion Channel Function in Sensory Transduction and Cellular Signaling Cascades. Boca Raton (FL): CRC Press/Taylor & Francis;* Frontiers in Neuroscience. Chapter 27.

86. Baratchi, S., Knoerzer, M., Khoshmanesh, K., Mitchell, A., McIntyre, P. (2017) Shear Stress Regulates TRPV4 Channel Clustering and Translocation from Adherens Junctions to the Basal Membrane. *Sci Rep.* 7, 15942.

87. Matthews, B.D., Thodeti, C.K., Tytell, J.D., Mammoto, A., Overby, D.R., Ingber, D.E. (2010) Ultra-rapid activation of TRPV4 ion channels by mechanical forces applied to cell surface beta1 integrins. *Integr Biol (Camb).* 2, 435-42.

88. Gilchrist, C.L., Leddy, H.A., Kaye, L., Case, N.D., Rothenberg, K.E., Little, D., Liedtke, W., Hoffman, B.D., Guilak, F. (2019) TRPV4-mediated calcium signaling in mesenchymal stem cells regulates aligned collagen matrix formation and vinculin tension. *Proc Natl Acad Sci U S A.* 116, 1992-1997.

89. Coste, B., Mathur, J., Schmidt, M., Earley, T.J., Ranade, S., Petrus, M.J., Dubin, A.E., Patapoutian, A. (2010) Piezo1 and Piezo2 are essential components of distinct mechanically activated cation channels. *Science.* 330, 55-60.

90. Brohawn, S.G., Campbell, E.B., MacKinnon, R. (2014) Physical mechanism for gating and mechanosensitivity of the human TRAAK K+ channel. *Nature.* 516, 126-30.

91. Vriens, J., Watanabe, H., Janssens, A., Droogmans, G., Voets, T., Nilius, B. (2004) Cell swelling, heat, and chemical agonists use distinct pathways for the activation of the cation channel TRPV4. *Proc Natl Acad Sci U S A.* 101, 396-401.

92. White, J.P., Cibelli, M., Urban, L., Nilius, B., McGeown, J.G., Nagy, I. (2016) TRPV4: Molecular Conductor of a Diverse Orchestra. *Physiol Rev.* 96, 911-73.

93. Toft-Bertelsen, T.L., Yarishkin, O., Redmon, S., Phuong, T.T.T., Križaj, D., MacAulay, N. (2019) Volume sensing in the transient receptor potential vanilloid 4 ion channel is cell type-specific and mediated by an N-terminal volume-sensing domain. *J Biol Chem.* 294, 18421-18434.

94. Berna-Erro, A., Izquierdo-Serra, M., Sepúlveda, R.V., Rubio-Moscardo, F., Doñate-Macián, P., Serra, S.A., Carrillo-Garcia, J., Perálvarez-Marín, A., González-Nilo, F., Fernández-Fernández, J.M., Valverde, M.A. (2017) Structural determinants of 5',6'-epoxyeicosatrienoic acid binding to and activation of TRPV4 channel. *Sci Rep.* 7, 10522.

95. Ryskamp, D.A., Jo, A.O., Frye, A.M., Vazquez-Chona, F., MacAulay, N., Thoreson, W.B., Križaj, D. (2014) Swelling and eicosanoid metabolites differentially gate TRPV4 channels in retinal neurons and glia. *J Neurosci.* 34, 15689-700.

96. Luna, C., Li, G., Qiu, J., Challa, P., Epstein, D.L., Gonzalez, P. (2009) Extracellular release of ATP mediated by cyclic mechanical stress leads to mobilization of AA in trabecular meshwork cells. *Invest Ophthalmol Vis Sci.* 50, 5805-10.

97. Zhou, L., Maruyama, I., Li, Y., Cheng, E.L., Yue, B.Y. (1999) Expression of integrin receptors in the human trabecular meshwork. *Curr Eye Res.* 19, 395-402.

98. Xiong, S., Xu, Y., Wang, Y., Kumar, A., Peters, D.M., Du, Y. (2020) α5β1 Integrin Promotes Anchoring and Integration of Transplanted Stem Cells to the Trabecular Meshwork in the Eye for Regeneration. *Stem Cells Dev.* 29, 290-300.

99. Filla, M.S., Faralli, J.A., Peotter, J.L., Peters, D.M. (2017) The role of integrins in glaucoma. *Exp Eye Res.* 158, 124-136.

100. Faralli, J.A., Filla, M.S., Peters, D.M. (2019) Effect of αvβ3 Integrin Expression and Activity on Intraocular Pressure. *Invest Ophthalmol Vis Sci.* 60, 1776-1788.

101. Rosenthal, R., Choritz, L., Schlott, S., Bechrakis, N.E., Jaroszewski, J., Wiederholt, M., Thieme, H. (2005) Effects of ML-7 and Y-27632 on carbachol- and endothelin-1-induced contraction of bovine trabecular meshwork. *Exp Eye Res.* 80, 837-45.

102. Sumida, G.M., Stamer, W.D. (2011) S1P receptor regulation of sphingosine-1-phosphate effects on conventional outflow physiology. *Am J Physiol Cell Physiol.* 300, C1164-71.

103. Boussommier-Calleja, A., Bertrand, J., Woodward, D.F., Ethier, C.R., Stamer, W.D., Overby, D.R. (2012) Pharmacologic manipulation of conventional outflow facility in ex vivo mouse eyes. *Invest Ophthalmol Vis Sci.* 53, 5838-45.

104. Yarishkin, O., Phuong, T.T.T., Bretz, C.A., Olsen, K.W., Baumann, J.M., Lakk, M., Crandall, A., Heurteaux, C., Hartnett, M.E., Križaj, D. (2018) TREK-1 channels regulate pressure sensitivity and calcium signaling in trabecular meshwork cells. *J Gen Physiol.* 150, 1660-1675.

105. Smith, M.A., Blankman, E., Deakin, N.O., Hoffman, L.M., Jensen, C.C., Turner, C.E., Beckerle, M.C. (2013) LIM domains target actin regulators paxillin and zyxin to sites of stress fiber strain. *PLoS One.* 8, e69378.

106. Deakin, N.O., Turner, C.E. (2008) Paxillin comes of age. *J Cell Sci.* 121, 2435-44.

107. Laudanna, C., Campbell, J.J., Butcher, E.C. (1996) Role of Rho in chemoattractant-activated leukocyte adhesion through integrins. *Science.* 271, 981-3.

108. Strotmann, R., Schultz, G., Plant, T.D. (2003) Ca2+-dependent potentiation of the nonselective cation channel TRPV4 is mediated by a C-terminal calmodulin binding site. *J Biol Chem.* 278, 26541-9.

109. Goswami, C., Kuhn, J., Heppenstall, P.A., Hucho, T. (2010) Importance of non-selective cation channel TRPV4 interaction with cytoskeleton and their reciprocal regulations in cultured cells. *PLoS One.* 5, e11654.

110. Murakoshi, H., Wang, H., Yasuda, R. (2011) Local, persistent activation of Rho GTPases during plasticity of single dendritic spines. *Nature.* 472, 100-4.

111. Tojkander, S., Ciuba, K., Lappalainen, P. (2018) CaMKK2 Regulates Mechanosensitive Assembly of Contractile Actin Stress Fibers. *Cell Rep.* 24, 11-19.

112. Wang, H., Chumnarnsilpa, S., Loonchanta, A., Li, Q., Kuan, Y.M., Robine, S., Larsson, M., Mihalek, I., Burtnick, L.D., Robinson, R.C. (2009) Helix straightening as an activation mechanism in the gelsolin superfamily of actin regulatory proteins. *J Biol Chem.* 284, 21265-9.

113. Bourguignon, L.Y., Gilad, E., Brightman, A., Diedrich, F., Singleton, P. (2006) Hyaluronan-CD44 interaction with leukemia-associated RhoGEF and epidermal growth factor receptor promotes Rho/Ras co-activation, phospholipase C epsilon-Ca2+ signaling, and cytoskeleton modification in head and neck squamous cell carcinoma cells. *J Biol Chem.* 281, 14026-40.

114. Rattan, S. (2017) Ca2+/calmodulin/MLCK pathway initiates, and RhoA/ROCK maintains, the internal anal sphincter smooth muscle tone. *Am J Physiol Gastrointest Liver Physiol.* 312, G63-G66.

115. Kirihara, T., Shimazaki, A., Nakamura, M., Miyawaki, N. (2014) Ocular hypotensive efficacy of Src-family tyrosine kinase inhibitors via different cellular actions from Rock inhibitors. *Exp Eye Res.* 119, 97-105.

116. Borrás, T. (2003) Gene expression in the trabecular meshwork and the influence of intraocular pressure. *Prog Retin Eye Res.* 22, 435-63.

117. Vittal, V., Rose, A., Gregory, K.E., Kelley, M.J., Acott, T.S. (2005) Changes in gene expression by trabecular meshwork cells in response to mechanical stretching. *Invest Ophthalmol Vis Sci.* 46, 2857-68.

118. Baetz, N.W., Hoffman, E.A., Yool, A.J., Stamer, W.D. (2009) Role of aquaporin-1 in trabecular meshwork cell homeostasis during mechanical strain. *Exp Eye Res.* 89, 95-100.

119. Bradley, J.M., Kelley, M.J., Rose, A., Acott, T.S. (2003) Signaling pathways used in trabecular matrix metalloproteinase response to mechanical stretch. *Invest Ophthalmol Vis Sci.* 44, 5174-81.

120. Adapala, R.K., Thoppil, R.J., Luther, D.J., Paruchuri, S., Meszaros, J.G., Chilian, W.M., Thodeti, C.K. (2013) TRPV4 channels mediate cardiac fibroblast differentiation by integrating mechanical and soluble signals. *J Mol Cell Cardiol.* 54, 45-52.

121. Sharma, S., Goswami, R., Zhang, D.X., Rahaman, S.O. (2019) TRPV4 regulates matrix stiffness and TGFβ1-induced epithelial-mesenchymal transition. *J Cell Mol Med.* 23, 761-774.

122. Goldhagen, B., Proia, A.D., Epstein, D.L., Rao, P.V. (2012) Elevated levels of RhoA in the optic nerve head of human eyes with glaucoma. *J Glaucoma.* 21, 530-8.

123. Yamamoto K, Maruyama K, Himori N, Omodaka K, Yokoyama Y, Shiga Y, Morin R, Nakazawa T. (2014) The novel Rho kinase (ROCK) inhibitor K-115: a new candidate drug for neuroprotective treatment in glaucoma. *Invest Ophthalmol Vis Sci.* 55, 7126-36.

124. Ryskamp, D.A., Witkovsky, P., Barabas, P., Huang, W., Koehler, C., Akimov, N.P., Lee, S.H., Chauhan, S., Xing, W., Rentería, R.C., Liedtke, W., Krizaj, D. (2011) The polymodal ion channel transient receptor potential vanilloid 4 modulates calcium flux, spiking rate, and apoptosis of mouse retinal ganglion cells. *J Neurosci.* 31, 7089-101.

125. Jo, A.O., Ryskamp, D.A., Phuong, T.T., Verkman, A.S., Yarishkin, O., MacAulay, N., Križaj, D. (2015) TRPV4 and AQP4 Channels Synergistically Regulate Cell Volume and Calcium Homeostasis in Retinal Müller Glia. *J Neurosci.* 35, 13525-37.

126. Krizaj, D., Lakk, M. (2019) Remodeling of focal adhesions and actin regulatory proteins in trabecular meshwork under tensile stress requires TRPV4-dependent Rho signaling *Invest. Ophthalmol. Vis. Sci.* 60, 5210.

127. Lakk, M., Young, D., Baumann, J.M., Jo, A.O., Hu, H., Križaj, D. (2018) Polymodal TRPV1 and TRPV4 Sensors Colocalize but Do Not Functionally Interact in a Subpopulation of Mouse Retinal Ganglion Cells. *Front Cell Neurosci.* 12, 353.

128. Lakk, M., Yarishkin, O., Baumann, J.M., Iuso, A., Križaj, D. (2017) Cholesterol regulates polymodal sensory transduction in Müller glia. *Glia.* 65, 2038-2050.

129. Lakk M and Krizaj D (2020) Mechanotransduction in trabecular meshwork cells requires obligatory interactions between TRPV4 channels, Rho signaling and focal adhesions. Annual ASBMB Meeting, San Diego. FASEB J 34(S1) 1-1.

Acknowledgements

Funding was provided by the National Institutes of Health (R01EY027920, P30EY014800), Glaucoma Research Foundation, Neuroscience Initiative at the University of Utah and an Unrestricted Grant from Research to Prevent Blindness to the Department of Ophthalmology at the University of Utah.

Figure Legends

Figure 1. Stretch-induced upregulation of actin cytoskeleton in human trabecular meshwork (hTM) cells requires TRPV4 and ROCK activation. (A) F-actin labeled with phalloidin- Alexa488 nm and (B) averaged data for TM cells. Preparations were stimulated with 1 hour 6% cyclic stretch in the presence/absence of TRPV4/ROCK inhibitors. Stretch-induced stress fiber increases were inhibited by HC-06 (1 µM) and Y-27632 (10 µM); exposure to the antagonists alone had no effect on stress fiber formation. Merged images are shown in panels on the right. Scale bar: 20 µm. *, $P < 0.05$, **, $P < 0.01$.

Figure 2. ROCK signaling is downstream from TRPV4. (A - C) Cytosolic Ca^{2+} signals (*left panel*s) and live actin fluorescence (*right panels*) were measured concurrently in Fura-2 AM-loaded cells. (A) GSK101 induced $[Ca^{2+}]_i$ elevations and reversibly stimulated stress fiber formation (panel ii) in the representative cell (n = 4). (Bi-iii) Y-27632 had no effect on baseline $[Ca^{2+}]_i$ but dissolved actin stress fibers in resting cell (n = 4). (Ci-iii) Y-27632 dissolves stress fibers without affecting the amplitude of GSK101-evoked $[Ca^{2+}]_i$ elevations (n = 4). (D) Averaged $[Ca^{2+}]_i$ data from Fura-2 AM-loaded cells (n = 52-162, N = 4). (E) Representative traces and averaged results for 30 min stretched (black trace, bars) and Y-27632-treated (10 µM, red trace, bars) TM cells. $[Ca^{2+}]_i$ responses induced by stretch are independent of Y-27632. ****, $P < 0.0001$; N.S., non-significant.

Figure 3. Stretch-induced stimulation of TRPV4 activates RhoA. (A) Semiquantitative RT-PCR, shown as ~fold *RhoA* mRNA following 1 – 7 hours of stretch. *RhoA* mRNA levels transiently increased after 1 hour biaxial stretch (3.00 ± 0.72; N = 4). (B & C) Western blot; active (GTP-bound) Rho protein

levels were increased at 1 hour stretch (1.56 ± 0.12; N = 3) whereas the inactive (GDP-bound) Rho levels were unaffected. HC-06 but not Y-27632, suppressed RhoA protein upregulation. *, $P < 0.05$.

Figure 4. TRPV4 and Rho-signaling time-dependently modulate stretch-induced phosphorylation of Focal Adhesion Kinase (FAK). (A) RT-PCR as ~fold *FAK* mRNA. Strain increases *FAK* mRNA levels at 3 hrs (1.57 ± 0.12-fold; N = 3). (B - D) Western blot data. (B) Total FAK protein levels remain constant, while FAK Tyr397 phosphorylation increases following 1 and 3 hour strain exposure (2.11 ± 0.07 and 2.28 ± 0.16, respectively; N = 3-5). (C & D) pFAK upregulation at 1 hour is inhibited by Y-27632 (0.88 ± 0.14; N = 3) but not HC-06, whereas 3 hour stretch effect is blocked by both antagonists (N = 3-5). *, $P < 0.05$, **, $P < 0.01$.

Figure 5. Stretch-induced paxillin phosphorylation requires TRPV4. (A) Semiquantitative RT-PCR, with ~fold changes of *paxillin* mRNA for 1 – 7 hour stretch (N = 3). (B - D) Western blots. (B) Stretch triggers an early elevation of activated (Tyr118) vs. nonactivated forms of the protein (N =3). (C) Western blot for total paxillin in control and stretched samples at 1-7 hours. (Di-ii) Western blot and averaged data for activated paxillin at 1 hour stretch, in the presence of HC-06, Y-27632 or BAPTA. The stretch effect is blocked by HC-06 and the calcium chelator BAPTA (N = 3). (E) Control (i) and stretched (ii) TM cells immunolabeled for p-paxillin, in the presence/absence of BAPTA (iii), HC-06 (iv), or Y-27632 (v). Stretch promotes the dispersal of p-paxillin towards distal membrane sites; TRPV4 and Rho inhibition lowers the extent and dispersion of active paxillin signals. (F) The number of p-paxillin (Tyr31) particuli is upregulated after 1 hour stretch in a TRPV4-, BAPTA- and ROCK-dependent manner, whereas the levels of total vinculin remain unchanged. (G) Colocalization between vinculin and p-paxillin increases in TRPV4- and Rho-dependent manner. *, $P < 0.05$, **, $P < 0.01$.

Figure 6. Biaxial stretch facilitates vinculin - pFAK colocalization. (A) Semiquantitative RT-PCR, ~fold changes of *vinculin* mRNA for 1 – 7 hour stretch durations. (B) Western blot. Stretch has no effect

on total vinculin protein levels. (C) Control and stretched TM cells in the presence/absence of HC-06 or Y-27632, immunolabeled for total vinculin and pFAK. Averaged data are shown in (D-G). 1 hour of stretch upregulates the (D & F) number of pFAK particuli in a ROCK-dependent manner, and increases the extent of colocalization with vinculin. (E & G) 3 hours of stretch increase pFAK levels and its colocalization with vinculin; this effect is blocked by both HC-06 and Y-27632. *, $P < 0.05$; **, $P < 0.01$; ***, $P < 0.001$. Scale bar: 20 µm.

Figure 7. Stretch-induced vinculin phosphorylation requires TRPV4 and Rho signaling. (A) Immunolabeling and averaged, normalized particulum size (B) for the total vinculin protein. (C) Immunolabeling and averaged, relative particulum number data (D) of Tyr1065-phosphorylated vinculin. Exposure to strain increases the p-vinculin particulum numbers at 1 hour together with the particulum size of total protein. These effects are suppressed by TRPV4 and ROCK inhibitors. N = 3; *, $P < 0.05$; **, $P < 0.01$. Scale bar: 20 µm.

Figure 8. TRPV4 and Rho-signaling time-dependently modulate stretch-induced phosphorylation of zyxin. (A) Semiquantitative RT-PCR. *Zyxin* mRNA is significantly increased at 1 - 5 hours stretch (N = 3-4). (B - E) Western blots. (B) Cyclic stretch triggers increases phosphorylated zyxin protein at 1 and 3 hours (N = 3-4). (Ci) Total zyxin protein in control and stretch samples at 1 – 7 hours. (Cii) Activated zyxin protein in the presence/absence of stretch and TRPV4/ROCK inhibition. Stretch augments zyxin/p-zyxin expression (D) Averaged data for experiments shown in Cii (N = 3-5). Stretch-induced upregulation in p-zyxin is suppressed by HC-06 and Y-27632 at 3 but not 1, hours. (Ei-ii) BAPTA-AM does not affect p-zyxin levels in the presence of stretch (N = 3). *, $P < 0.05$; **, $P < 0.01$; N.S. = non-significant.

Figure 9. Mechanical force-induced translocation of zyxin requires TRPV4 and Rho signaling. Double labeling for F-actin and total zyxin. 1- hour stretch increases zyxin-ir shows diminished localization, promotes translocation into stress fibers but reduces overall FA zyxin localization. Stretch-

induced translocation of zyxin is inhibited by HC-06 and Y-27632, in the presence of which zyxin favors membrane locations (N = 3). Stretched Y-27632 but not HC-06-treated cells also show zyxin expression in the perinuclear area (N = 3). Scale bar: 20 µm.

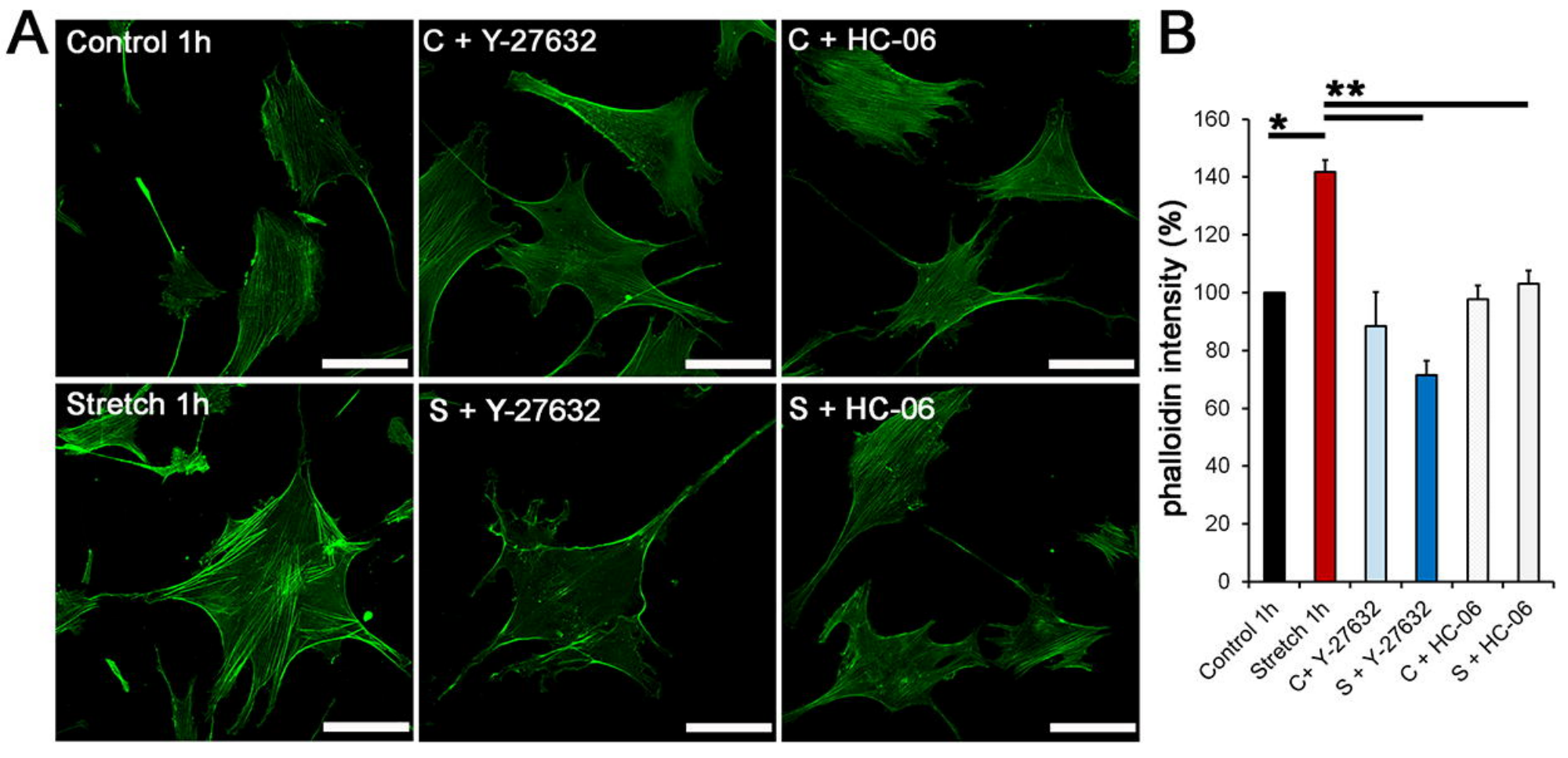
A
Control 1h
C + Y-27632
C + HC-06
Stretch 1h
S + Y-27632
S + HC-06
B
*
**
phalloidin intensity (%)
160
140
120
100
80
60
40
20
0
Control 1h
Stretch 1h
C+ Y-27632
S + Y-27632
C + HC-06
S + HC-06

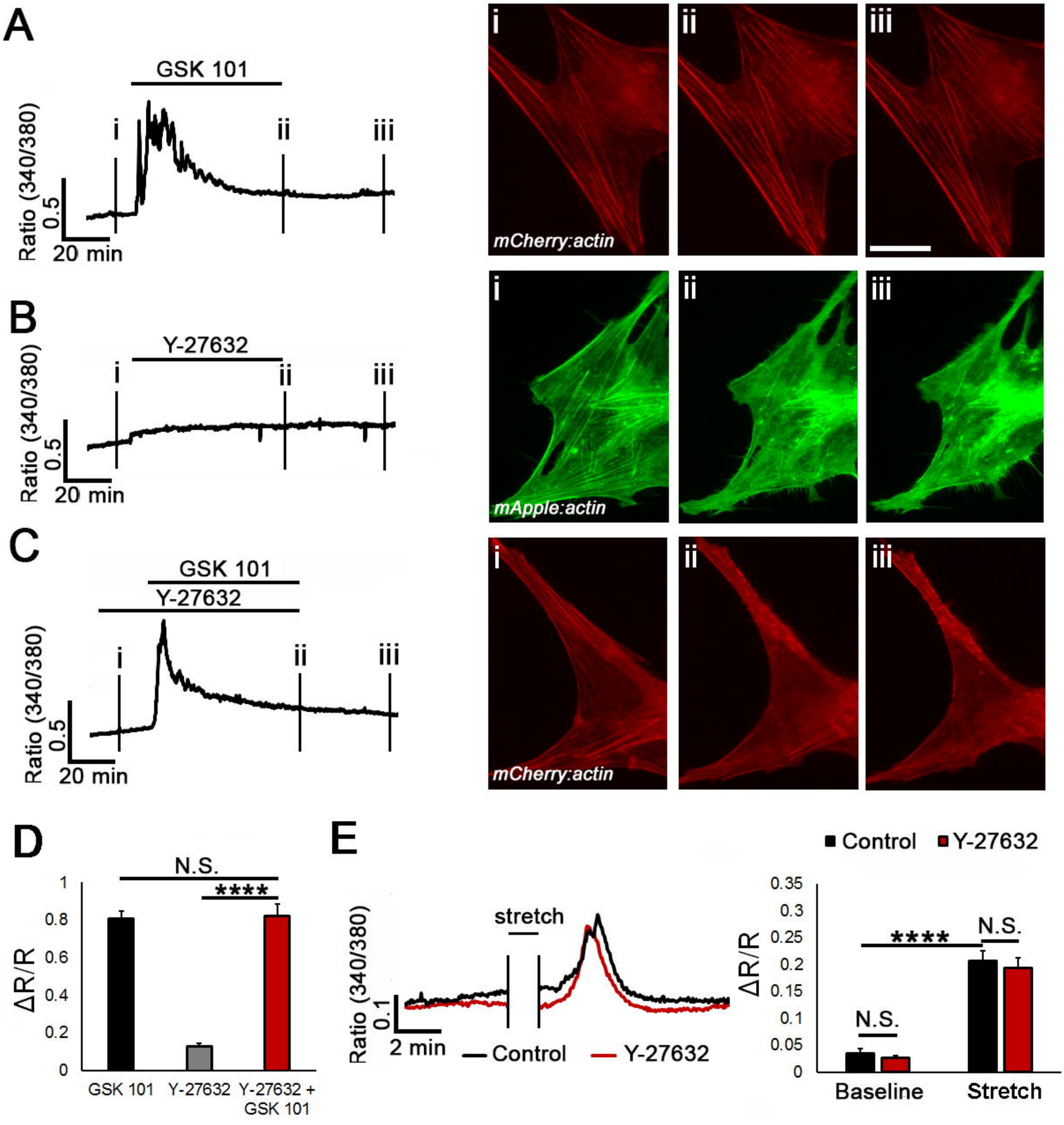
A
GSK 101
i
ii
iii
Ratio (340/380)
0.5
20 min
mCherry:actin
B
Y-27632
mApple:actin
C
GSK 101
Y-27632
D
N.S.
****
ΔR/R
GSK 101
Y-27632
Y-27632 + GSK 101
E
Control
Y-27632
stretch
2 min
Baseline
Stretch

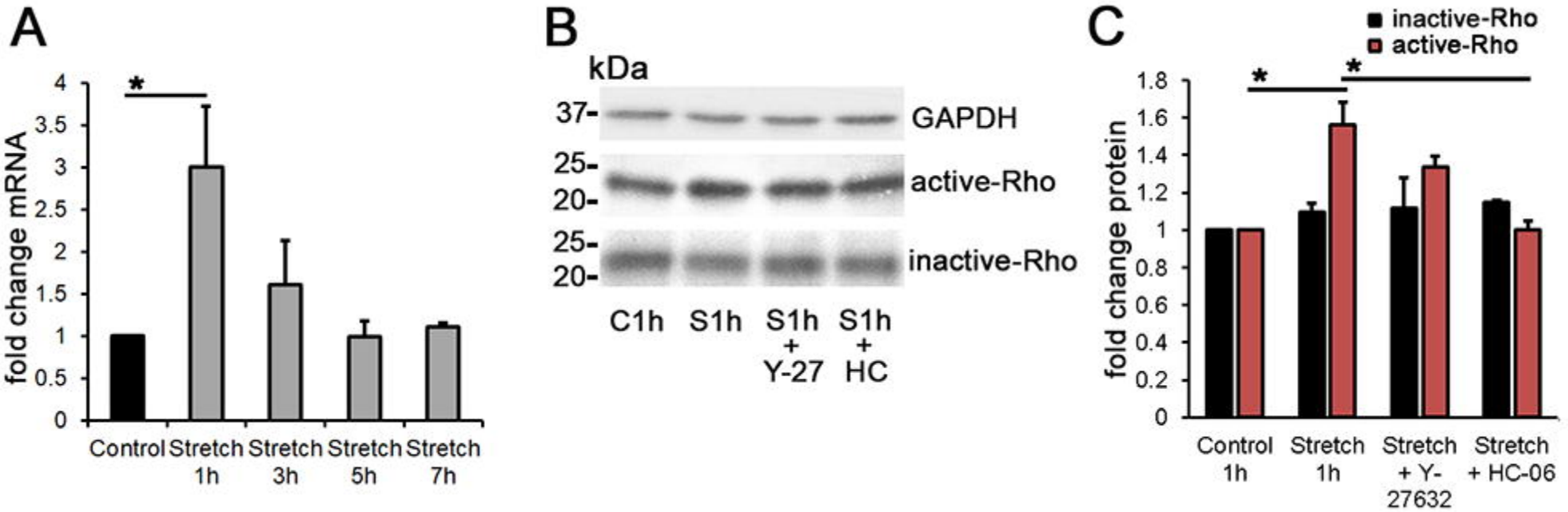
A
fold change mRNA
4
3.5
3
2.5
2
1.5
1
0.5
0
*
Control
Stretch 1h
Stretch 3h
Stretch 5h
Stretch 7h
B
kDa
37-
25-
20-
25-
20-
GAPDH
active-Rho
inactive-Rho
C1h
S1h
S1h + Y-27
S1h + HC
C
inactive-Rho
active-Rho
fold change protein
1.8
1.6
1.4
1.2
1
0.8
0.6
0.4
0.2
0
*
*
Control 1h
Stretch 1h
Stretch + Y-27632
Stretch + HC-06

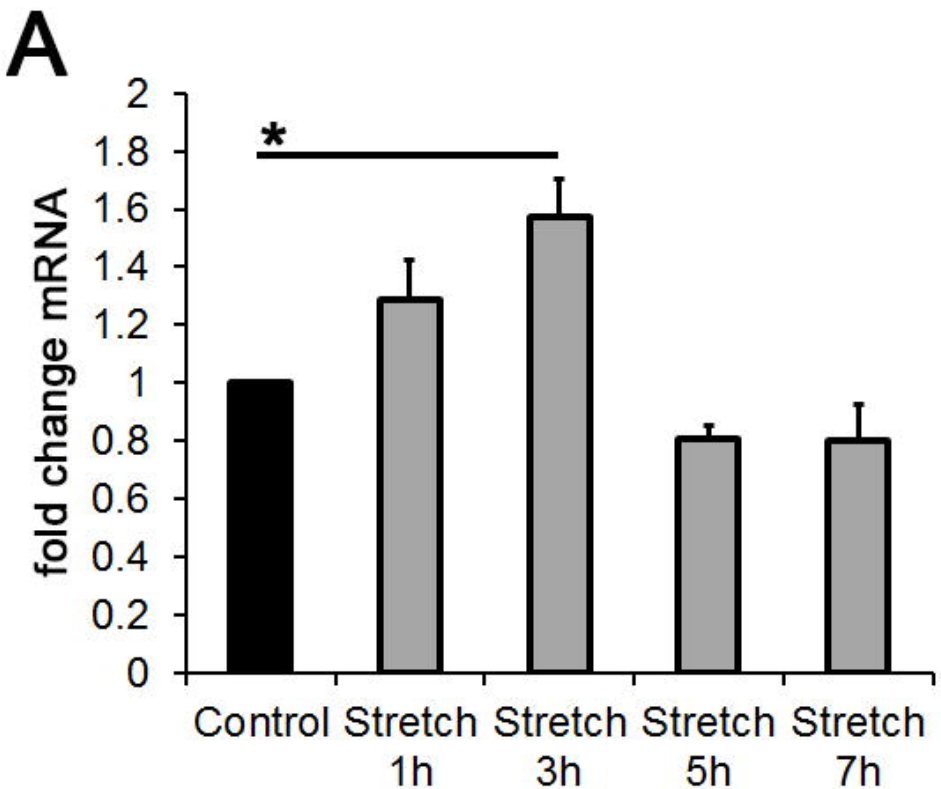
A
fold change mRNA
2
1.8
1.6
1.4
1.2
1
0.8
0.6
0.4
0.2
0
*
Control
Stretch 1h
Stretch 3h
Stretch 5h
Stretch 7h

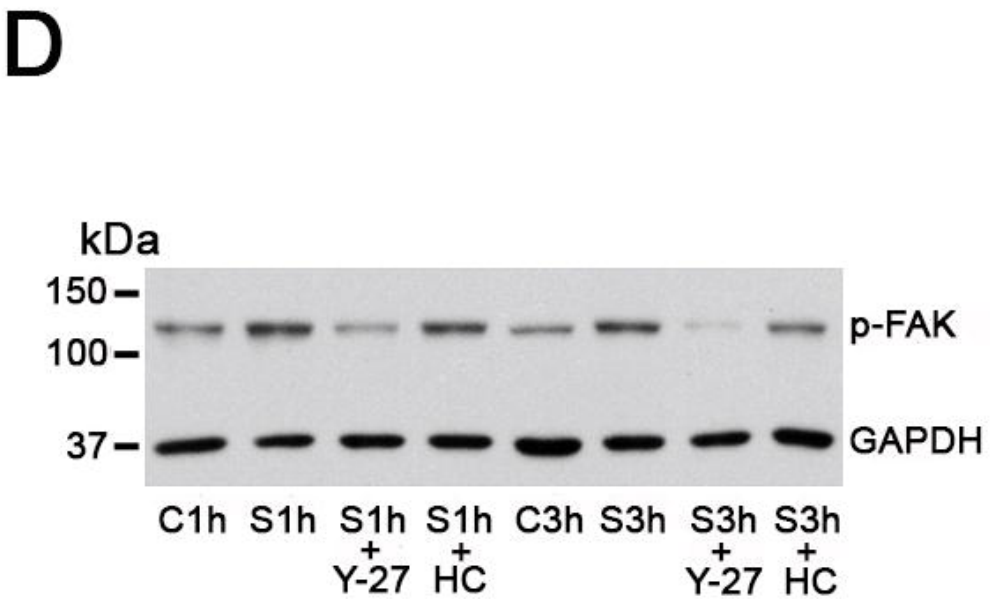
D
kDa
150
100
37
p-FAK
GAPDH
C1h
S1h
S1h + Y-27
S1h + HC
C3h
S3h
S3h + Y-27
S3h + HC

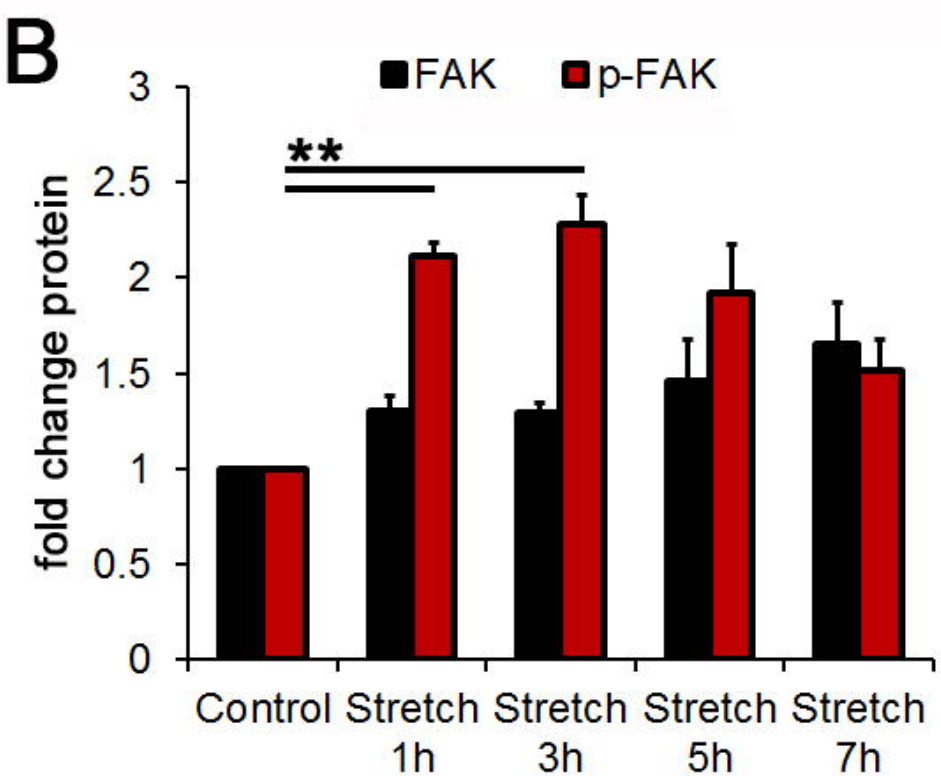
B
FAK
p-FAK
fold change protein
3
2.5
2
1.5
1
0.5
0
**
Control
Stretch 1h
Stretch 3h
Stretch 5h
Stretch 7h

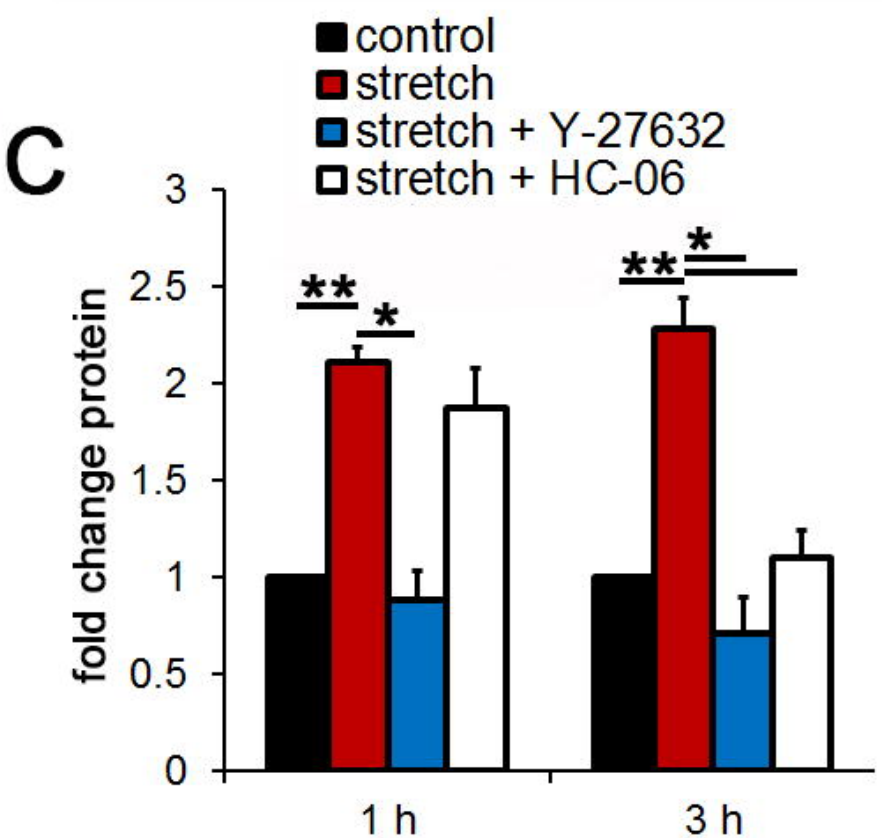
C
control
stretch
stretch + Y-27632
stretch + HC-06
fold change protein
3
2.5
2
1.5
1
0.5
0
**
*
**
*
1 h
3 h

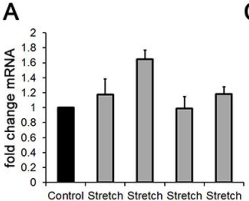
A
fold change mRNA
Control
Stretch 1h
Stretch 3h
Stretch 5h
Stretch 7h

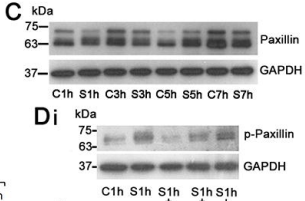
C
kDa
75
63
37
Paxillin
GAPDH
C1h S1h C3h S3h C5h S5h C7h S7h
Di
p-Paxillin
GAPDH
C1h S1h S1h + BAPTA S1h + HC S1h + Y-27
ii
fold change protein
Control 1h
Stretch 1h
S + BAPTA
S + HC-06
S + Y-27632

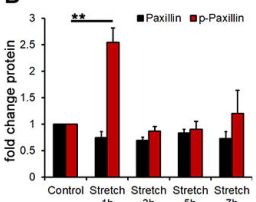
B
Paxillin
p-Paxillin
fold change protein
Control
Stretch 1h
Stretch 3h
Stretch 5h
Stretch 7h

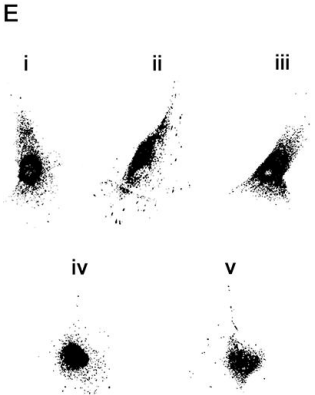
E
i
ii
iii
iv
v

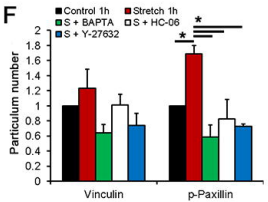
F
Control 1h
Stretch 1h
S + BAPTA
S + HC-06
S + Y-27632
Particulum number
Vinculin
p-Paxillin

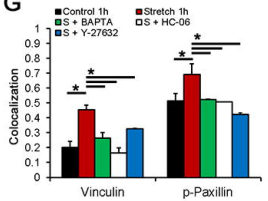
G
Control 1h
Stretch 1h
S + BAPTA
S + HC-06
S + Y-27632
Colocalization
Vinculin
p-Paxillin

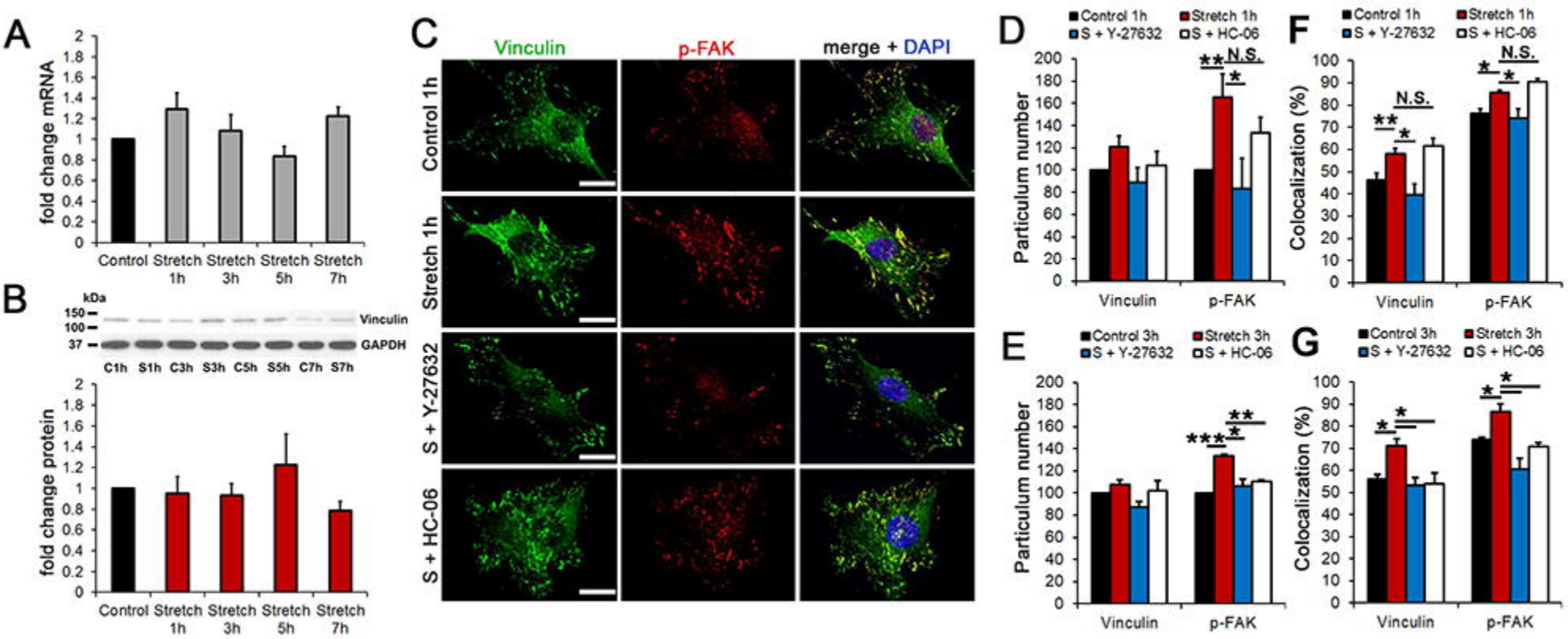
A
fold change mRNA
Control
Stretch 1h
Stretch 3h
Stretch 5h
Stretch 7h
B
kDa
150
100
37
Vinculin
GAPDH
C1h S1h C3h S3h C5h S5h C7h S7h
fold change protein
C
Vinculin
p-FAK
merge + DAPI
Control 1h
Stretch 1h
S + Y-27632
S + HC-06
D
Control 1h
Stretch 1h
S + Y-27632
S + HC-06
Particulum number
N.S.
Vinculin
p-FAK
E
Control 3h
Stretch 3h
S + Y-27632
S + HC-06
Particulum number
Vinculin
p-FAK
F
Control 1h
Stretch 1h
S + Y-27632
S + HC-06
Colocalization (%)
N.S.
Vinculin
p-FAK
G
Control 3h
Stretch 3h
S + Y-27632
S + HC-06
Colocalization (%)
Vinculin
p-FAK

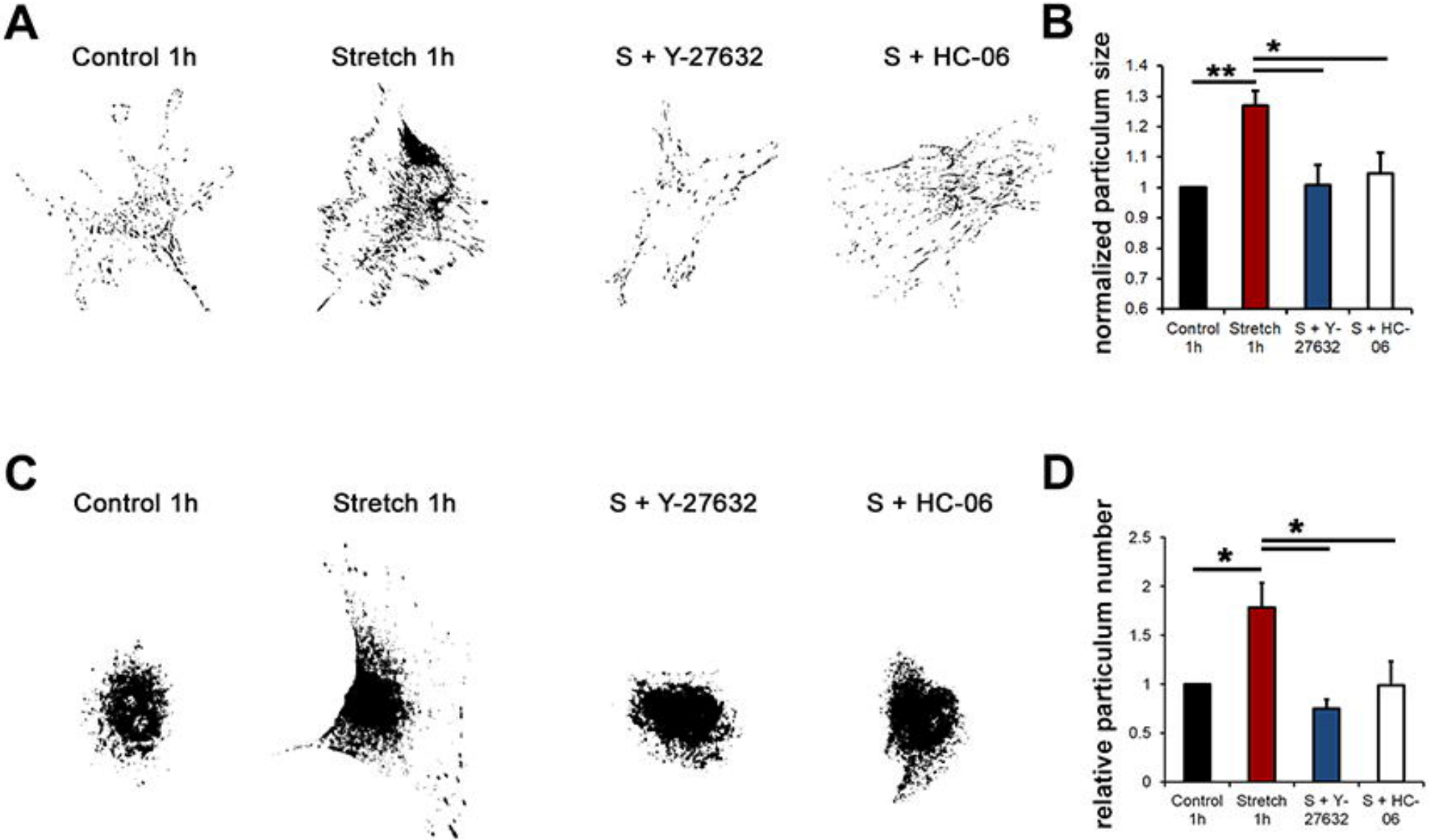
A
Control 1h
Stretch 1h
S + Y-27632
S + HC-06
B
normalized particulum size
1.4
1.3
1.2
1.1
1
0.9
0.8
0.7
0.6
**
*
Control 1h
Stretch 1h
S + Y-27632
S + HC-06
C
Control 1h
Stretch 1h
S + Y-27632
S + HC-06
D
relative particulum number
2.5
2
1.5
1
0.5
0
*
*
Control 1h
Stretch 1h
S + Y-27632
S + HC-06

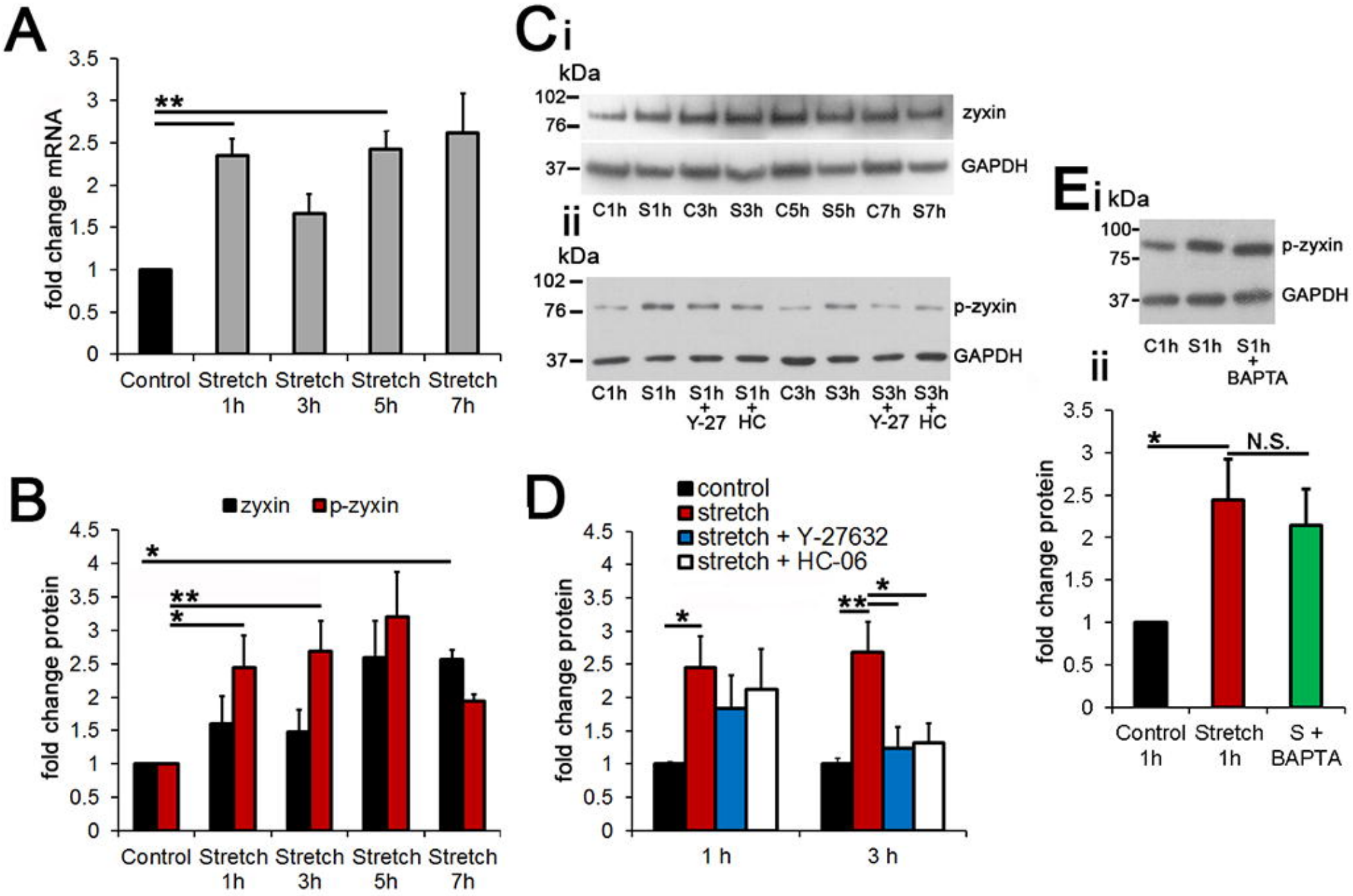
A
fold change mRNA
3.5
3
2.5
2
1.5
1
0.5
0
**
Control
Stretch 1h
Stretch 3h
Stretch 5h
Stretch 7h
Ci
kDa
102
76
37
zyxin
GAPDH
C1h S1h C3h S3h C5h S5h C7h S7h
ii
kDa
102
76
37
p-zyxin
GAPDH
C1h S1h S1h + Y-27 S1h + HC C3h S3h S3h + Y-27 S3h + HC
Ei
kDa
100
75
37
p-zyxin
GAPDH
C1h S1h S1h + BAPTA
ii
fold change protein
*
N.S.
Control 1h
Stretch 1h
S + BAPTA
B
zyxin
p-zyxin
fold change protein
4.5
4
3.5
3
2.5
2
1.5
1
0.5
0
*
**
*
Control
Stretch 1h
Stretch 3h
Stretch 5h
Stretch 7h
D
control
stretch
stretch + Y-27632
stretch + HC-06
fold change protein
*
**
*
1 h
3 h

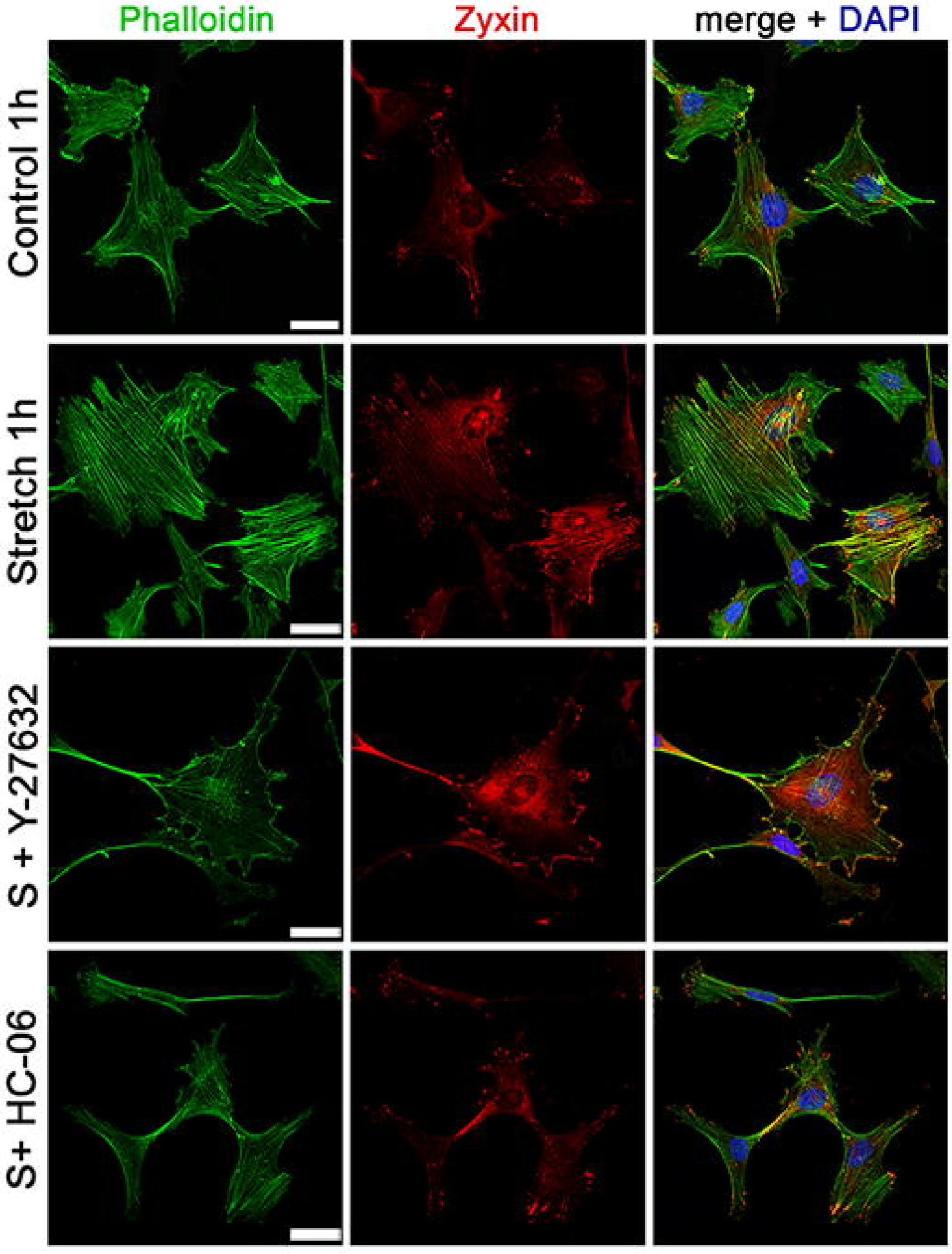
Phalloidin
Zyxin
merge + DAPI
Control 1h
Stretch 1h
S + Y-27632
S+ HC-06